TIME-FREQUENCY DOMAIN ANALYSIS OF VIBRATION SIGNALS FOR MACHINERY DIAGNOSTICS
(I) INTRODUCTION TO THE WIGNER-VILLE DISTRIBUTION

by

P.D.McFADDEN and W.WANG

Report No. OUEL 1859/90

University of Oxford
Department of Engineering Science
Parks Road
Oxford
OX1 3PJ
U.K.

Tel. (0865) 273000
FAX (0865) 273010

ABSTRACT

This report reviews the definition and some of the properties of the Wigner-Ville distribution for both continuous and discrete signals. A digital computer program implementing the discrete Wigner-Ville distribution is described and its performance is demonstrated by the analysis in the time-frequency domain of a series of numerically-generated test signals, showing the form of the Wigner-Ville distribution and the interference terms which can be generated due to its non-linear behaviour. The program is then applied to the analysis in the time-frequency domain of experimentally-measured time domain averages of the vibration of damaged gears in industrial and helicopter gearboxes, in order to detect early signs of impending mechanical failure. It is shown that the damage to the gears can be detected by visual inspection of the changes which occur in the pattern of the Wigner-Ville distribution, but that the damage can be detected more quickly and easily using an existing narrow band enhancement technique.

CONTENTS

1. INTRODUCTION

The Wigner-Ville distribution (WVD) provides a powerful means of representing a given signal in the time-frequency domain. The original formulation was found more than 60 years ago by Wigner and Szilard, and it was Wigner [1] who first introduced it in 1932 into the field of quantum mechanics, where the probability-function of the simultaneous values of coordinates and momenta was calculated. Ville [2] proposed its use in signal analysis in 1948 when he defined the analytical signal. Several other representations were defined from time to time between the 1940s and the 1960s [3,4]. In 1966 Cohen [5] proposed a general formulation for joint time-frequency distributions which provided a comprehensive framework for the study and understanding of the many representations which, previously, had been narrowly defined.

To perform digital computation of the distribution, it is necessary to have a discrete definition of the WVD. Claasen and Mecklenbräuker [6] proposed a criterion for selecting the most appropriate time-frequency distribution for engineering applications which provides an unbiased estimate of the instantaneous frequency of the signal with the best resolution and accuracy in the time-frequency domain when applied to a mono-component frequency modulation (FM) signal. They suggested several definitions of the discrete WVD, but the properties of the continuous WVD were not preserved due to aliasing effects. Chan [7] proposed what he called "a non-aliased discrete-time Wigner distribution", but still failed to resolve completely the problem of aliasing. The reasons for the various definitions and whether or not they suffer from aliasing errors were not clearly discussed until Peyrin and Prost [8] presented a "unified definition for the discrete-time, discrete-frequency and discrete-time/frequency" Wigner distribution. Their definition of the discrete WVD is directly related to the corresponding continuous definition and so preserves most of its useful properties. The aliasing problem is also discussed sufficiently.

The recent rise in interest in the WVD stems from its applicability to several engineering signal processing problems, although the actual application of the WVD in engineering seems to have come rather late, with the work of Bouachache et al [9,10] in the late 1970s. In recent years, the WVD has been applied in various areas of signal analysis, such as speech processing and image processing, and it is also considered to be of particular interest for non-stationary signal analysis. It has been suggested that the WVD should be applied to the detection and analysis of the vibration signals from rotating machinery, in which periodic signals, due for example to the normal meshing of gears, may be modulated

by the changes to the vibration produced by one or more teeth as the degree of localized damage increases.

In the field of machinery diagnostics, several simple digital processing techniques have been developed over the last decade and a half and applied to the enhancement of the time domain averages of gearbox vibration signals [11–16]. Some of these techniques concentrate on a narrow band of the frequency spectrum, usually centred on the dominant harmonic of the tooth meshing frequency [12–16]. It can be shown that the enhanced signals produced by these techniques represent the amplitude and phase modulation of the tooth meshing vibration by the effects of the tooth damage [13]. It has even been suggested that the location of the damage to a gear tooth may be identified from the phase information produced by one of these techniques [15,16]. The potential weaknesses of these narrow band techniques are obvious. Firstly, only a part of the information contained in the frequency spectrum is being utilized, with the consequent risk that information important for the detection of a damaged tooth on a gear may be missed. Secondly, in cases of severe gear damage, impulsive signals having a broad frequency spectrum may become increasingly important, and these impacts may not necessarily be centred at one of the tooth meshing harmonics [17]. While the narrow band techniques have proved effective in many instances, the investigation of alternative analytical methods is highly desirable.

Forrester [18,19] has made a significant contribution to machinery diagnostics by applying the WVD to the analysis of the time domain averages of the vibration of helicopter gearboxes. He has suggested that the WVD is capable of distinguishing between a variety of faults, such as tooth cracking and pitting, which previously required the use of specialized analysis procedures. However, a detailed explanation of the often complicated WVD patterns observed and a full discussion of exactly how these patterns should be interpreted in order to distinguish between different types of faults in gears has not been given.

This report reviews the definitions for the continuous WVD and some of its useful properties. The selection of a suitable definition for the discrete WVD is then considered together with the problem of aliasing errors. An implementation of the discrete WVD on a digital computer is then described, and the performance of the implementation is demonstrated by the analysis of a variety of numerically-generated test signals. The performance of the implementation is then evaluated for several experimentally-derived time domain averages of the vibration signals from industrial and helicopter gearboxes, and compared with the results of the existing narrow band enhancement techniques.

2. THE WIGNER AND WIGNER-VILLE DISTRIBUTIONS

2.1 Definition of the Wigner Distribution

Let $x(t)$ be a continuous complex signal. The Wigner distribution (WD) of the signal $x(t)$ is defined [1] as

$$W_x(t,f) = \int_{-\infty}^{+\infty} x\left(t+\frac{\tau}{2}\right)\, x^*\left(t-\frac{\tau}{2}\right)\, \exp\left(-j2\pi f\tau\right) d\tau \tag{1}$$

where * denotes complex conjugation. If $X(f)$ is the Fourier transform of $x(t)$, an equivalent definition is

$$W_X(f,t) = \int_{-\infty}^{+\infty} X\left(f+\frac{\eta}{2}\right)\, X^*\left(f-\frac{\eta}{2}\right)\, \exp\left(j2\pi t\eta\right) d\eta. \tag{2}$$

By this definition, a symmetric role in time and frequency domain exists, given by

$$W_x(t,f) = W_X(f,t). \tag{3}$$

2.2 Properties of the Wigner Distribution

The WD possesses a number of useful properties which have been extensively studied [6]. The following properties are fundamental.

Property 1: *The WD is a real function.*

$$W_x(t.f) \in \Re \tag{4}$$

Property 2: *The instantaneous signal power is equal to the projection of the WD on the time axis and the spectral density is equal to the projection on the frequency axis.*

$$\int_{-\infty}^{+\infty} W_x(t,f)\, df = |x(t)|^2 \tag{5a}$$

$$\int_{-\infty}^{+\infty} W_x(t,f)\, dt = |X(f)|^2 \tag{5b}$$

Property 3: *The WD is reversible up to a constant factor.*

$$\int_{-\infty}^{+\infty} W_x\left(\frac{t}{2},f\right) \exp\left(j2\pi ft\right) df = x(t)\, x^*(0) \tag{6a}$$

$$\int_{-\infty}^{+\infty} W_x\left(t, \frac{f}{2}\right) \exp\left(-j2\pi ft\right) dt = X(f)\, X^*(0) \tag{6b}$$

Property 4: *The WD of the product of two signals is equal to the convolution of the WDs of each signal with respect to frequency. The WD of the convolution of two signals is equal to the convolution of the WDs of each signal with respect to time.*

$$W_{xy}(t,f) = \int_{-\infty}^{+\infty} W_x(t,v)\, W_y(t, f-v)\, dv \tag{7a}$$

$$W_{x*y}(t,f) = \int_{-\infty}^{+\infty} W_x(\tau, f)\, W_y(t-\tau, f)\, d\tau \tag{7b}$$

As the signal $x(t)$ is complex, it can be represented as

$$x(t) = x_R(t) + j\, x_I(t) \tag{8}$$

where $x_R(t)$ and $x_I(t)$ are the real and imaginary parts of the signal respectively. The integrand function $V(t,\tau)$ is given by

$$\begin{aligned} V(t,\tau) &= V_R(t,\tau) + j\, V_I(t,\tau) \\ &= x\left(t+\frac{\tau}{2}\right)\, x^*\left(t-\frac{\tau}{2}\right). \end{aligned} \tag{9}$$

where $V_R(t,\tau)$ and $V_I(t,\tau)$ are the real and imaginary parts of the function respectively. It is easily shown that

$$V_R(t,\tau) = x_R\left(t+\frac{\tau}{2}\right) x_R\left(t-\frac{\tau}{2}\right) + x_I\left(t+\frac{\tau}{2}\right) x_I\left(t-\frac{\tau}{2}\right) \tag{10a}$$

$$V_I(t,\tau) = x_I\left(t+\frac{\tau}{2}\right) x_R\left(t-\frac{\tau}{2}\right) - x_R\left(t+\frac{\tau}{2}\right) x_I\left(t-\frac{\tau}{2}\right). \tag{10b}$$

Property 5: *The real and imaginary parts of the integrand function are even and odd functions respectively with respect to τ.*

$$V_R(t,-\tau) = V_R(t,\tau) \tag{11a}$$

$$V_I(t,-\tau) = -V_R(t,\tau) \tag{11b}$$

2.3 Definition of the Wigner-Ville Distribution

Consider the case where $x(t)$ is an analytical signal. The imaginary part $x_I(t)$ is equal to the Hilbert transform of the real part $x_R(t)$, so that

$$x_I(t) = \frac{1}{\pi} \int_{-\infty}^{+\infty} \frac{x_R(\tau)}{t-\tau}\, d\tau. \tag{12}$$

For the case where $x(t)$ is an analytical signal, the Wigner distribution is termed the Wigner-Ville distribution [2].

3. THE DISCRETE WIGNER-VILLE DISTRIBUTION

3.1 Definition of the Discrete Wigner-Ville Distribution

Let function $x(t)$ represent a continuous periodic signal with period NT. Let $\widehat{x}(t)$ be a sampled version of the continuous signal $x(t)$ with sampling period T. The sampled signal can be expressed as

$$\widehat{x}(t) = \sum_{k=0}^{N-1} x(kT)\,\delta(t - kT) \tag{13}$$

where δ represents the Dirac function. Let the sampling rate in the frequency domain be Λ. Thus by using equation (1)

$$\begin{aligned} W_{\widehat{x}}(t,f) &= \frac{1}{2NT}\int_{-\infty}^{+\infty}\left[\sum_{k=0}^{N-1} x(kT)\,\delta\left(t+\frac{\tau}{2}-kT\right)\right]\left[\sum_{n} x(nT)\,\delta\left(t-\frac{\tau}{2}-nT\right)\right] \\ &\qquad\cdot\left[\sum_{m}\exp\left(-j2\pi\tau\ m\Lambda\right)\delta(f-m\Lambda)\right]d\tau \\ &= \frac{1}{2NT}\sum_{n}\sum_{m}\left[\sum_{k=0}^{N-1} x(kT)\,x^{*}(nT)\,\exp\left(-j2\pi(k-n)Tm\Lambda\right)\right] \\ &\qquad\cdot\,\delta\left(t-(k+n)\frac{T}{2}\right)\,\delta(f-m\Lambda). \end{aligned} \tag{14}$$

Since $x(kT)$ has period of NT, let $n' = k + n$ so that

$$\begin{aligned} W_{\widehat{x}}(t,f) &= \frac{1}{2NT}\sum_{n'}\sum_{m}\left[\sum_{k=0}^{N-1} x(kT)\,x^{*}\left((n'-k)T\right)\,\exp\left(-j2\pi(2k-n')Tm\Lambda\right)\right] \\ &\qquad\cdot\,\delta\left(t-\frac{n'T}{2}\right)\,\delta(f-m\Lambda). \end{aligned} \tag{15}$$

It is clear that the WVD of the sampled signal is sampled in time at a rate twice that of the signal. For consistency, the sampling rates in time and frequency must satisfy the relationship

$$\Lambda = \frac{1}{2NT}. \tag{16}$$

Thus by writing n' as n

$$\begin{aligned} W_{\widehat{x}}(t,f) &= \frac{1}{T}\sum_{n}\sum_{m}\left[\frac{1}{2N}\sum_{k=0}^{N-1} x(kT)\,x^{*}\left((n-k)T\right)\,\exp\left(-j\frac{\pi\ m(2k-n)}{N}\right)\right] \\ &\qquad\cdot\,\delta\left(t-\frac{nT}{2}\right)\,\delta\left(f-\frac{m}{2NT}\right). \end{aligned} \tag{17}$$

The discrete WVD $W(n,m)$ is defined as

$$W(n,m) = \frac{1}{2N} \sum_{k=0}^{N-1} x(kT)\, x^*\big((n-k)T\big)\, \exp\left(-j\frac{\pi m(2k-n)}{N}\right). \tag{18}$$

The following relationship relates the definition for the discrete WVD to the definition for continuously sampled signals.

$$W_{\widehat{x}}(t,f) = \frac{1}{T} \sum_{n,m} W(n,m)\, \delta\left(t - \frac{nT}{2}\right)\, \delta\left(f - \frac{m}{2NT}\right) \tag{19}$$

It is easy to verify that $W(n,m)$ is a periodic function of period $2N$ in both time and frequency. It can be shown that

$$W(n+Np, m+Nq) = (-1)^{pm+qn+Npq}\, W(n,m) \tag{20}$$

where p and q are integers. Considering the case where $p,q = 0,1$ gives

$$\begin{aligned} W(n+N,m) &= (-1)^m\, W(n,m) \\ W(n,m+N) &= (-1)^n\, W(n,m) \\ W(n+N,m+N) &= (-1)^{m+n+N}\, W(n,m). \end{aligned} \tag{21}$$

The last three relationships show that in the range $(0 \le n < 2N-1)$, $(0 \le m < 2N-1)$, representing one complete period, the WVD need only be calculated over the range $(0 \le n < N-1)$, $(0 \le m < N-1)$, having an area of one quarter that of the complete period. If the absolute value of the WVD is taken, it is seen from equation (20) that

$$\mid W(n+Np, m+Nq) \mid = \mid W(n,m) \mid . \tag{22}$$

If one period is considered by taking $(0 \le n < N-1)$, $(0 \le m < N-1)$, and $p,q = 0,1$, the absolute value of the WVD will repeat in both time and frequency domains. That is, in the following four areas the regional WVD patterns are completely the same.

$$\begin{aligned} &(0 \le n < N-1), (0 \le m < N-1) \\ &(N \le n < 2N-1), (0 \le m < N-1) \\ &(0 \le n < N-1), (N \le m < 2N-1) \\ &(N \le n < 2N-1), (N \le m < 2N-1) \end{aligned}$$

3.2 Aliasing in the Discrete Wigner-Ville Distribution

It can be proved [8] that $W(n,m)$ is the superposition of four components of the continuous function $W_x(t,f)$, given by

$$W(n,m) = \frac{1}{4NT}\left[W_x\left(\frac{nT}{2},\frac{m}{2NT}\right) + (-1)^n W_x\left(\frac{nT}{2},\frac{m-N}{2NT}\right)\right.$$
$$\left.+(-1)^m W_x\left((n+N)\frac{T}{2},\frac{m}{2NT}\right) + (-1)^{n+m+N} W_x\left((n+N)\frac{T}{2},\frac{m-N}{2NT}\right)\right]. \quad (23)$$

Therefore in order to obtain an aliasing-free discrete WVD, the corresponding continuous WVD should satisfy the following conditions

$$W_x(t,f) = 0 \qquad \text{for} \qquad f<0, \quad f>\frac{1}{2T} \quad (24a)$$

and

$$W_x(t,f) = 0 \qquad \text{for} \qquad t<0, \quad t>\frac{NT}{2}. \quad (24b)$$

From the first condition, considering Property 2, it is seen that

$$\int_{-\infty}^{+\infty} W_x(t,f)\,dt = |X(f)|^2 = 0 \qquad \text{for} \qquad f<0, \quad f>\frac{1}{2T} \quad (25)$$

therefore

$$X(f) = 0 \qquad \text{for} \qquad f<0, \quad f>\frac{1}{2T} \quad (26a)$$

and, similarly, the second condition can be satisfied by

$$x(t) = 0 \qquad \text{for} \qquad t<0, \quad t>\frac{NT}{2}. \quad (26b)$$

This means that if the maximum frequency and time length of the signal do not exceed $1/2T$ and $NT/2$ respectively, aliasing can be completely avoided in the WVD. In practice, conditions (24a) and (24b) can only *approximately* be satisfied simultaneously.

3.3 Computation of the Discrete Wigner-Ville Distribution

For convenience of calculation, the even and odd time samples may be separated, replacing n with $2n$ and $2n+1$ respectively in equation (18), to obtain for the even time samples

$$W(2n,m) = \frac{1}{2N}\sum_{k=0}^{N-1} x\big((n+k)T\big)\,x^*\big((n-k)T\big)\,\exp\left(-j\frac{2\pi mk}{N}\right) \quad (27a)$$

and for the odd time samples

$$W(2n+1,m) = \frac{1}{2N} \exp\left(j\frac{\pi m}{N}\right) \sum_{k=0}^{N-1} x\big((n+k)T\big)\, x^*\big((n-k+1)T\big) \exp\left(-j\frac{2\pi mk}{N}\right). \quad (27b)$$

It is clear that the above discrete WVD can be calculated by the FFT. The WVD for a complete period of $2N$ points requires N FFTs each of length N, $N/2$ FFTs for the even time samples and $N/2$ FFTs, multiplied by a factor of $\exp(j\pi m/N)$, for the odd time samples.

4. IMPLEMENTATION

4.1 The Computer System

The discrete WVD has been implemented on an IBM PC-AT compatible computer with 80386 processor and 80387 maths co-processor running at 20 MHz, a 70 Mbyte fixed disc and a VGA graphics monitor. All programs have been written in Microsoft C under the MS-DOS operating system. Extensive use has been made of a user-friendly interface controlled entirely by a three-button mouse and featuring screen buttons, fields and popup menus. Where possible, existing library functions have been used for operations such as the calculation of the Fourier transform of the time domain average, the calculation of the Hilbert transform, and routine file-based input and output operations.

4.2 The Computer Program

The computer program operates as follows. The required time domain average, typically comprising 1024 real samples, is read from the appropriate file on the hard disc and the corresponding analytical signal calculated using the Hilbert transform, with interpolation being performed by zero-padding of the top end of the spectrum so that the final analytical signal consists of 4096 complex sample pairs.

The user may select the required starting angle of rotation within the limits ± 360 degrees and the range of rotation angle from the range 360, 180, 90 or 45 degrees. The range of rotation angle specified is then scanned in 256 passes. For the first pass with $n = 0$, the product $x((n+k)T)\,x^*((n-k)T)$ as presented in equation (27a) is formed for values of k from 0 to 4095. A block size specified by the user from the range 512, 1024 or 2048 determines the size of the increment of k. By using a larger block size and hence a smaller increment, the resolution of the WVD in the frequency domain may be improved at the expense of increased computation time. The forward Fourier transform of the product is then calculated using an FFT routine to yield the WVD for that value of n, consisting of an array of 257, 513 or 1025 real values, depending upon the selected block size.

At this stage, the user may choose to pre-scale the values in the array by calculating the absolute value, or the positive or negative parts only and setting the remainder to zero, or the logarithm of one of these. The pre-scaled array is then converted to an array of integer values in the range 0 to 15, corresponding to a palette of 16 colours in accordance with upper and lower amplitude limits specified by the user. The colours are then written

to the screen as a line of 512 pixels over the range of frequencies specified by the user. The process is then repeated for the next value of n, eventually producing a display 512 pixels wide by 256 pixels high.

EGA 16-colour high-resolution graphics mode was chosen for the display as it offers a resolution of 640 pixels wide by 350 pixels high, giving a large work area for the WVD while leaving sufficient room for the necessary axis labels and annotation. VGA 16-colour high-resolution graphics mode provides a resolution of 640 pixels wide by 480 pixels high, but to take advantage of the extra vertical resolution, more than 256 values of n must be used, and there is no suitable value which is also radix 2. By choosing the size of the Fourier transform, the range of frequencies to be displayed across the horizontal axis and the range of rotation angles to be displayed along the vertical axis, the user has considerable control over the compromise between execution time and resolution. A grey-scale hard copy of the WVD may be produced by laser printer.

The execution time for a WVD using a block size of 1024 samples, including the time taken for the calculation of the analytical function but without logarithmic pre-scaling, is 210 seconds.

5. NUMERICAL EXAMPLES

5.1 Selection of Relevant Examples

The examples in this section are intended to demonstrate some of the basic features of the WVD for the types of signals which are likely to be found in the experimentally-measured time domain averages of the vibration produced by gears in industrial and helicopter gearboxes. The examples have been generated numerically by computer programs written in Microsoft C, and take the form of time domain averages each containing 1024 samples.

The vibration signal produced by a normal gear consists primarily of the fundamental and harmonics of the tooth meshing frequency. The relative amplitudes of these components depends upon the exact tooth profile and upon the transfer function between the tooth contact region and the location of the vibration transducer, which is usually mounted on the casing of the gearbox. In practice, small variations between the gear teeth due to manufacturing errors produce small fluctuations in the vibration signal. These give rise to modulation sidebands in the frequency spectrum of the time domain average spaced at intervals of the rotation frequency from the tooth meshing components.

The changes in the vibration produced by localized damage to a gear, such as a spall on the surface of one tooth or a small fatigue crack, also give rise to modulation sidebands in the frequency spectrum, clustered around the harmonics of the tooth meshing frequency [20]. When the damage to a gear tooth is extensive, the very large and rapid changes in the tooth force may excite resonances in the gearbox which can be measured by the vibration transducer. In the frequency spectrum of the time domain average, a resonance may sometimes be identified as a cluster of components rising above the level of the modulation sidebands at a frequency well separated from the harmonics of the tooth meshing frequency [17].

Thus to demonstrate the application of the WVD to gear vibration signals, examples have been selected which show the amplitude and phase modulation of periodic signals, the summation of several periodic signals of which some are harmonically related, and time-limited periodic signals.

5.2 Example N1 Unmodulated Sine Wave

Figure 1(a) shows a numerically-generated test signal consisting of an unmodulated sine wave of unit amplitude and frequency of 48 orders. The WVD for this signal, presented

in Figure 1(b), shows a single dark line at 48 orders against a mid-grey background corresponding to an amplitude of zero.

5.3 Example N2 Amplitude Modulated Sine Wave

Figure 2(a) shows a test signal consisting of a sine wave of unit amplitude and frequency 48 orders amplitude modulated at the 75% level by a cosine wave of frequency 2 orders. In Figure 2(b), the WVD shows a line at 48 orders varying in intensity, surrounded by modulation sidebands of varying intensity, against a mid-grey background corresponding to a level of zero. Several sidebands are present, although the first-order sidebands are by far the largest. Note that the upper and lower first-order sidebands change in unison from a positive amplitude, shown as dark grey, where the level of the test signal is a maximum, to a negative amplitude, shown as pale grey, where the level is a minimum. A linear intensity scale has been used here to show correctly the changes in the level of the modulation sidebands.

5.4 Example N3 Phase Modulated Sine Wave

Figure 3(a) presents a test signal consisting of a sine wave of unit amplitude and frequency 48 orders phase modulated at 360 degrees by a sine wave of frequency 2 orders. The phase shift of the test signal is 0 degrees at 0, 90, 180, 270 and 360 degrees of rotation. The maximum phase advance of 360 degrees occurs at 45 and 225 degrees, and the maximum lag of -360 degrees occurs at 135 and 315 degrees.

The WVD for this signal appears in Figure 3(b). For small angles, phase modulation is linear [21], so produces only first-order sidebands. However, phase modulation at 360 degrees is non-linear, so that many modulation sidebands appear in the WVD, although the first-order sidebands are the largest in this example. At 0 and 180 degrees of rotation, when the phase shift is 0 degrees and increasing, the first upper sideband has a large positive value and appears as a black line, while the first lower sideband has a negative value and appears as a white line. At 90 and 270 degrees of rotation, when the phase shift is again 0 degrees but is decreasing, the sign of these sidebands is reversed. At 45, 135, 225 and 315 degrees, where the maximum phase deviations occur, the level of the modulation sidebands in the WVD falls to zero and the level of the component at 48 orders reaches its maximum value. From this example it is clear that great care must be taken when interpreting sideband patterns in the WVD which are produced by phase modulation.

5.5 Example N4 Sum of Sine Waves

Figure 4(a) shows a test signal consisting of the sum of sine waves of unit amplitude at frequencies of 32, 48 and 96 orders. The WVD of this signal in Figure 4(b) features dark grey lines at 32, 48 and 96 orders corresponding to these components, as well as dashed lines, alternating between black and white, at 40, 64 and 72 orders. These dashed lines arise from interference between the given components. The line at 40 orders lies midway between the lines at 32 and 48 orders, and the dashed pattern repeats at 16 orders, the difference in frequency between the lines. Similarly the dashed lines at 64 and 72 orders arise from the interference between the lines at 32 and 48 orders respectively and the line at 96 orders, and have repeat frequencies of 32 and 48 orders respectively.

The time domain average for a gearbox may contain periodic signals at the tooth meshing frequency and its harmonics. Hence interference lines may be expected in the WVD at the frequencies midway between the harmonics of the tooth meshing frequency. The interference line between every second harmonic will coincide with the line produced by the intervening meshing harmonic, so causing it to have a dashed appearance also. Furthermore, if a ghost component is present, interference lines will be produced midway between the ghost frequency and each of the meshing harmonics.

5.6 Example N5 Tone Burst

Figure 5(a) shows a test signal comprising a tone burst consisting of three cycles of a sine wave at 48 orders, having a smoothly tapering sinusoidal envelope of unit maximum amplitude, beginning at 90 degrees of rotation.

The WVD for the signal is shown in Figure 5(b). In order to reveal the extent of the patterns in the WVD present at very low levels, a logarthmic conversion has been applied. A broad grey band is centred at 48 orders and extending across the range from below 32 orders to above 64 orders. This band is produced by the tone burst itself. A similar band, but with alternating vertical stripes, occurs at the same frequency 180 degrees later. The test signal is periodic in 360 degrees of rotation, so this second band is due to the interference between the original band and its neighbour in the following rotation. In the previous example, the interference between lines having different frequencies at the same instant in time was noted. In this example, interference is seen between lines having the same frequencies but occuring at different times.

5.7 Example N6 Sum of Tone Burst and Sine Wave

Figure 6(a) shows a test signal comprising the sum of a pure sine wave of unit amplitude and frequency 48 orders and the tone burst described in the previous example. The signal is intended to be representative of the type of short-duration change in the vibration produced by damage to a single tooth on a gear.

The WVD for this test signal is shown in Figure 6(b). A logarithmic conversion has been applied to reveal the changes in the pattern of the WVD at low levels. A black line is visible at 48 orders corresponding to the sine wave. The dark band produced by the tone burst is also visible between 32 and 64 orders beginning at 90 degrees of rotation, as well as the interference band 180 degrees of rotation later. In addition, a pattern of broad curved bands has appeared due to the interference between the sine wave and the tone burst. The separation of the bands decreases with increasing distance from the location of the tone burst.

6. EXPERIMENTAL EXAMPLES

6.1 Example E1 Ball Mill Gearbox

The time domain averages presented in this section were obtained from one of a series of large reduction gearboxes, each containing three double-helical gears, which drive ball mills for the pulverizing of coal in a power station. The input gear, driven by an electric motor, has 28 teeth which mesh with the 64 teeth on an idler gear. The idler gear also meshes with the output gear having 175 teeth. The gearbox has a height of approximately 3 metres.

Accelerometers were fitted on the bearing caps on the shafts on either side of the gearbox. The output of each accelerometer was integrated to give a signal proportional the the velocity, which was then recorded on magnetic tape. A synchronizing signal comprising one pulse per revolution of the input shaft, obtained from an inductive sensor placed near the keyway on the input shaft, was also recorded. Time domain averages for the input, idler and output gears were calculated for several gearboxes by interpolation [22].

Figure 7(a) shows the time domain average obtained for the idler gear in one of the gearboxes. The pattern of vibration at the tooth meshing frequency is clearly visible, together with an abrupt change in the level of vibration at approximately 210 degrees. Figure 7(b) presents the enhanced time domain average calculated by applying the narrow band enveloping technique [12] about the fundamental tooth meshing frequency,showing a large peak at the location of the tooth damage. The normalized fourth statistical moment, known as the kurtosis, provides a simple measure of the importance of the peaks in a signal. The kurtosis of the enhanced time domain average is 6.8, which is outside the range of 2.5 to 3.5 which might be expected for an undamaged gear. During the subsequent visual inspection of the gear, a small spall was discovered on one tooth face.

The WVD for the time domain average of this gear is shown in Figure 7(c). The pattern is relatively complicated, with a solid vertical line corresponding to the tooth meshing frequency at 64 orders and a dashed vertical line due to a ghost component at 180 orders, together with many other dashed vertical lines. Some of these are produced by the interference between the meshing harmonics and the ghost. Others arise because the numbers of teeth on the input and idler gears have a common factor of four, so that modulation sidebands are produced at multiples of $64/4 = 16$ orders. There is a clear disturbance in the pattern of the distribution at approximately 210 degrees, corresponding to the position of the peak in Figure 7(b), spreading over the range from 48 orders to

76 orders. Figure 7(d) presents the WVD calculated from the time domain average from which all harmonics of the tooth meshing frequency had first been eliminated. The change in the pattern of the distribution at 210 degrees is now clearer, as many of the vertical lines caused by the interference have been removed. A small change in the pattern can also be seen in the range 160 to 180 orders. Strong lines at 48 and 80 orders due to the modulation at 16 orders remain. The dashed line at 64 orders corresponds to interference between the lines at 48 and 80 orders.

6.2 Example E2 Helicopter Input Spiral Bevel Gear

The time domain averages presented in this section were obtained by Westland Helicopters Limited using a full-scale back-to-back test facility for the main rotor gearbox of a Wessex helicopter undergoing fatigue testing [23]. During testing at very high load, a fatigue crack began at the root of one of the teeth in the input spiral bevel pinion and progressed along the length of the tooth.

Figure 8(a) shows the time domain average obtained when the fatigue crack was still small. The gear has 22 teeth, but due to the method of mounting the accelerometer on the gearbox, the dominant component of the time domain average is the fourth harmonic of the tooth meshing frequency at 88 orders. Applying the narrow band envelope technique [12] about the dominant fourth harmonic of the tooth meshing frequency at 88 orders gives the enhanced time domain average presented in Figure 8(b), with a large peak at approximately 270 degrees revealing the presence of the damage. The kurtosis of the enhanced time domain average is 9.9, indicating with certainty that the gear is damaged.

The WVD for this time domain average is presented in Figure 8(c). The relatively high level of noise across the spectrum of this time domain average produces a complicated pattern, but a disturbance can be seen at approximately 270 degrees between 64 and 96 orders and in the high frequency region between 160 and 192 orders. If all of the harmonics of the tooth meshing frequency are removed from the time domain average gives the WVD in Figure 8(d) is obtained. The distribution has now been simplified, so that the changes in the pattern are more readily identified.

6.3 Example E3 Helicopter Epicyclic Planet Gear

In the early 1980s the Royal Aircraft Establishment at Farnborough conducted a series of tests on the main rotor gearbox of a Whirlwind helicopter to assess the ability of current

techniques of vibration analysis to detect damage to epicyclic gear systems [24]. As a part of this series of tests, a Whirlwind gearbox was dismantled and a part of one of the teeth on one of the planet gears in the first epicyclic stage of the gearbox was ground off at one end. The gearbox was reassembled and tested under load in a back-to-back test facility. Tape recordings were made of the vibration at seven locations on the gearbox. A synchronizing signal from a sensor on the input shaft was also recorded. These tape recordings have now been analyzed using a technique which enables the time domain averages for the individual planet gears and the sun gear to be extracted from the total vibation of an epicyclic gearbox [25–28].

Figure 9(a) shows the time domain average for one of the planet gears obtained from the recordings for test number P2, for which 30% of one tooth had been removed. The pattern of tooth meshing vibration at 21 orders is clearly visible, together with higher harmonics, particularly the second. Figure 9(b) presents the enhanced time domain average [14] for the gear obtained about the dominant second harmonic of the tooth meshing frequency, with a broad peak being visible at approximately 315 degrees. The enhanced time domain average has a kurtosis of 5.3, confirming the departure of the signal from that expected for a normal gear.

The WVD of the time domain average is given in Figure 9(c). Solid vertical lines are present at the first three harmonics of the tooth meshing frequency, together with fainter lines at many intermediate frequencies as a result of interference between the meshing harmonics. Note in particular that the second and third harmonics at 42 and 63 orders are dashed, as they coincide with the interference components arising from the meshing harmonics on either side of them. The change in the pattern near 315 degrees produced by the damaged tooth is very minor, consisting of faint curved lines in the range 21 to 42 orders. Figure 9(d) shows the WVD for the time domain average from which all the harmonics of the tooth meshing frequency have been eliminated. The pattern is now much clearer, and with only two strong vertical lines remaining at 20 and 22 orders corresponding to first order modulation sidebands, the changes in the ranges 21 to 42 orders and 84 to 105 orders are easily seen.

7. DISCUSSION

7.1 Comparison with Other Enhancement Techniques

When Forrester [19] proposed that the WVD may be suitable for the early detection of failure in mechanical systems, he claimed that the existing narrow band techniques for the enhancement of time domain averages had two major drawbacks. Firstly, the selective filtering or removal of part of the time domain average is required. Secondly, the enhanced time domain average can accurately portray only those signals in which the average frequency content does not vary with time. Forrester claimed [19] that, with most tooth faults, both the amplitude and the frequency content of the vibration signal will change during the time that the damaged part of a gear is in mesh, and that in consequence, the WVD, with its representation of the signal in the time-frequency domain, should give a superior description of the condition of a gear.

The three examples in the previous section have demonstrated that the WVD can be applied to the early detection of failure in mechanical systems. However, in each example the damage to the gear could be more clearly detected in the graph produced by the existing narrow band envelope enhancement technique than in the time-frequency domain representation produced by the WVD. No special judgement was required in the application of the narrow band technique, as in each case the centre frequency selected was that harmonic of the tooth meshing frequency which had the greatest amplitude. The kurtosis of the enhanced time domain average gave an unequivocal indication in each example that gear damage was present.

Comparison of the execution times of the narrow band envelope enhancement technique and the WVD is instructive. The former requires less than 3 seconds, while for a high-resolution WVD more than 210 seconds are required, even when using a high-speed personal computer with maths co-processor.

7.2 Removal of Meshing Harmonics

One of Forrester's arguments in favour of the WVD for the analysis of gear vibration is that no selective filtering or removal of parts of the time domain average is necessary. Certainly the WVD can be calculated from the original time domain average, but as indicated in this report, the WVD is inherently non-linear due to the product term $x(kT)\,x^*((n-k)T)$. The vibration signal produced by the meshing of a normal gear typically contains large

periodic components at the tooth meshing frequency and its harmonics. Interference between these components caused by the non-linearity of the WVD gives rise to the patterns of dashed lines at the sum and difference frequencies, shown clearly in Figures 7(c) and 9(c). While these lines can immediately be identified as interference components by their dashed appearance, they do add an unnecessary complication to the WVD. The purpose of an enhancement technique is to simplify the representation of a vibration signal in such a way that subtle changes in the vibration can be detected more readily and hence give earlier warning of incipient failure. In the form proposed by Forrester, the WVD, by introducing additional features into the representation of the signal for an undamaged gear, seems to run counter to this aim.

The vibration at the tooth meshing frequency and its harmonics contains no information which can assist in the detection of tooth damage, except for the provision of a reference level with which the level of the vibration at other frequencies may be compared. Any variation in the vibration from one tooth to the next can be deduced from the modulation sidebands surrounding the meshing components, or from the excitation of resonances at other frequency ranges [17]. The regular components at the harmonics of the tooth meshing frequency in the time domain average describe the vibration signature of the average tooth on the gear, so that the elimination of these components leaves simply the departures of the individual gear teeth from the average [14], sometimes referred to as the residual signal [11]. The WVD of the residual signal should therefore be easier to interpret than the WVD of the original time domain average because the meshing components have been removed, together with the interference components associated with them.

The WVDs shown in Figures 7(d), 8(d) and 9(d) demonstrate this improvement clearly. The removal of the interference components makes the change in the pattern due to the tooth damage more obvious. This is particularly important in the case of the Whirlwind planet gear, as the change in the pattern of the WVD for the original time domain average shown in Figure 9(c) is very slight. The WVD for the residual signal presented in Figure 9(d) gives a much clearer indication of the damage.

The vibration signals produced by practical geared systems are often complicated, containing several harmonics of the tooth meshing frequency, modulation sidebands and sometimes ghost components. While the concept of a universally-applicable analysis technique which can detect damage to a gear with no prior knowledge of the design of that gear may be attractive, the reality is that any additional information about the gear which

is available can significantly affect the standard of the diagnosis. Only in the rarest of circumstances will the analyst be required to examine a gear system in which the numbers of teeth on the gears are not known. The theory behind the elimination of the tooth meshing components is well understood [14] and the technique is easily applied. The results presented in this report provide a clear case for the calculation of the WVD of the residual signal, as well as if not instead of the WVD of original time domain average.

7.3 Forrester's Examples

Forrester [18] has provides four examples of the time domain averages of damaged gears, comparing the ability of the WVD and the narrow band envelope enhancement technique to detect the damage. In the first two examples, it is shown that both techniques can detect different stages of development of a fatigue crack in the input spiral bevel gear of the main rotor gearbox of a Wessex helicopter. The third example concerns the detection of spalling damage to the teeth of another Wessex input spiral bevel pinion. Again, both techniques are able to detect the damage.

In his fourth example, Forrester has considered the time domain average produced by the epicyclic planet gear in a Brevini gearbox, with a small flat ground off one tooth of the gear. The damage is shown clearly in the WVD, but the kurtosis for the time domain average after enhancement by the narrow band envelope technique is quoted as only 3.7, suggesting that the technique has failed to detect the damage [18]. However, using the same data, it has been shown that a kurtosis of 10.3 can be obtained for this time domain average by applying the narrow band technique with a centre frequency equal to the tooth meshing frequency of 32 orders and a bandwidth of ± 15 orders [29]. Clearly, the narrow band technique *can* detect the damage to the gear. A possible explanation for the discrepancy is that Forrester has used a different centre frequency.

8. CONCLUSIONS

This report has reviewed the definition and some of the properties of the continuous WVD and the definition of the discrete WVD. A digital computer program implementing the discrete WVD has been described. The program has been demonstrated using several numerically-generated test signals to illustrate the forms of the WVD for pure and modulated sine wave signals and to show the interference terms which can be generated due to the non-linear nature of the WVD. The program has been applied to the analysis of the experimentally-measured time domain averages of the vibration of damaged gears in industrial and helicopter gearboxes. It has been shown that in each example the damage to the gear can be detected from the changes to the pattern of the WVD, but that the damage could have been detected more quicky and easily, and without the need for visual inspection, using an existing narrow band enhancement technique.

It has been shown that the changes in the pattern of the WVD for a damaged gear are enhanced if the regular components at the tooth meshing frequency and its harmonics are first eliminated from the time domain average. This has the very important effect of removing from the WVD not only the meshing harmonics but also the interference components which occur between them.

This report has demonstrated that the WVD can be used in the early detection of mechanical failure in gear systems, but on the basis of its performance in the examples considered, the WVD, in its present form, cannot compete with existing enhancement techniques.

ACKNOWLEDGEMENTS

The authors wish to thank the Science and Engineering Research Council for its support of this research, the Mechanical Research Division of Westland Helicopters Limited for permission to use the Wessex helicopter data, and the Naval Aircraft Materials Laboratory for making available the Whirlwind helicopter data.

REFERENCES

1. E.WIGNER 1932 *Physical Review* **40**, 749–759. On the quantum correction for thermodynamic equilibrium.
2. J.VILLE 1948 *Cables et Transmission* **194**(1), 61–74. Théorie et application de la notion de signal analytique.
3. D.GABOR 1946 *IEEE Journal*, London, **93**. Theory of communication.
4. C.H.PAGE 1953 *Journal of Applied Physics* **23**(1), 103–106. Instantaneous power spectra.
5. L.COHEN 1966 *Journal of Mathematical Physics* **7**(5), 781–786. Generalized phase-space distribution functions.
6. T.A.C.M.CLAASEN and W.F.G.MECKLENBRÄUKER 1980 *Philips Journal of Research* **35**, 217–250. The Wigner distribution – a tool for time-frequency signal analysis. Part I: Continuous-time signals.
7. D.S.K.CHAN 1982 *Proceedings ICASSP*, Paris, France, 1333–1336. A non-aliased discrete-time Wigner distribution for time-frequency signal analysis.
8. F.PEYRIN and R.PROST 1986 *IEEE Transactions on Acoustics Speech and Signal Processing* **ASSP34**(4), 858–867. A unified definition for the discrete-time, discrete-frequency, and discrete-time/frequency Wigner distributions.
9. B.BOUACHACHE et al 1978 *Publication ELF-Aquitaine, No 373/78, Pau, France.* Représentation temps-fréquence.
10. B.BOUACHACHE 1979 *Comptes Rendus Acad. Sciences* **288**A, 307–309. Sur une condition nécessaire et suffisante de positivité de la représentation conjointe en temps et fréquence des signaux d'énergie finite.
11. R.M.STEWART 1977 *Institute of Sound and Vibration Research, Paper MHM/R/-10/77.* Some useful data analysis techniques for gearbox diagnostics.
12. P.D.McFADDEN and J.D.SMITH 1985 *Proceedings of the Institution of Mechanical Engineers* **199**(C4), 287–292. A signal processing technique for detecting local defects in a gear from the signal average of the vibration.
13. P.D.McFADDEN 1986 *ASME Transactions Journal of Vibration Acoustics Stress and Reliability in Design* **108**(2), 165–170. Detecting fatigue cracks in gears by amplitude and phase demodulation of the meshing vibration.
14. P.D.McFADDEN 1987 *Mechanical Systems and Signal Processing* **1**(2), 173–183. Examination of a technique for the early detection of failure in gears by signal processing

of the time domain average of the meshing vibration.

15. P.D.McFADDEN 1988 *Mechanical Systems and Signal Processing* **2**(4), 403–409. Determining the location of a fatigue crack in a gear from the phase of the change in the meshing vibration.
16. P.D.McFADDEN 1989 ***Department of Engineering Science, University of Oxford, Report OUEL 1751/89.*** The effect of load on the tooth meshing vibration of a spiral bevel gear with a small fatigue crack.
17. P.D.McFADDEN 1985 *NDT International* **18**(5) 279–282. Low frequency vibration generated by gear tooth impacts.
18. B.D.FORRESTER 1990 *Proceedings of the 44th Meeting of the Mechanical Failures Prevention Group of the Vibration Institute*, Virginia Beach, Virginia, April 3–5, 225–234. Analysis of gear vibration in the time-frequency domain.
19. B.D.FORRESTER 1990 *Aeronautical Research Laboratory, ARL Propulsion Report 180, Melbourne, Australia.* Time-frequency domain analysis of helicopter transmission vibration.
20. R.B.RANDALL 1982 *ASME Transactions Journal of Mechanical Design* **104**, 259–267. A new method of modelling gear faults.
21. A.B.CARLSON 1975 *Communication Systems*, second edition, pp 181–183, 240–241. McGraw-Hill, New York.
22. P.D.McFADDEN 1989 *Mechanical Systems and Signal Processing* **3**(1), 87–97. Interpolation techniques for time domain averaging of gear vibration.
23. M.J.STUCKEY 1981 *Westland Helicopters Limited, Mechanical Research Report MR-R20019.* Wessex main rotor gearbox (MOD 1762) fatigue test - vibration monitoring - trial no. 3 (final).
24. P.J.LEGGE 1984 *Royal Aircraft Establishment, Technical Report 84064.* Vibration health monitoring of epicyclic gearboxes.
25. P.D.McFADDEN 1989 *Department of Engineering Science, University of Oxford, Report OUEL 1747/88.* A technique for calculating the time domain averages of the vibration of the individual planet gears in an epicyclic gearbox.
26. P.D.McFADDEN 1989 *Department of Engineering Science, University of Oxford, Report OUEL 1752/89.* A technique for calculating the time domain average of the vibration of the sun gear in an epicyclic gearbox.
27. P.D.McFADDEN 1990 *Department of Engineering Science, University of Oxford, Re-*

port OUEL 1818/90. The selection of weighting functions for the calculation of time domain averages of the vibration of the individual gears in an epicyclic gearbox.

28. P.D.McFADDEN 1990 *Journal of Sound and Vibration* (To be published.) A technique for calculating the time domain averages of the vibration of the individual planet gears and the sun gear in an epicyclic gearbox.
29. P.D.McFADDEN and I.M.HOWARD 1990 *Aeronautical Research Laboratory, ARL Propulsion Report 183, Melbourne, Australia.* The detection of seeded faults in an epicyclic gearbox by signal averaging of the vibration.

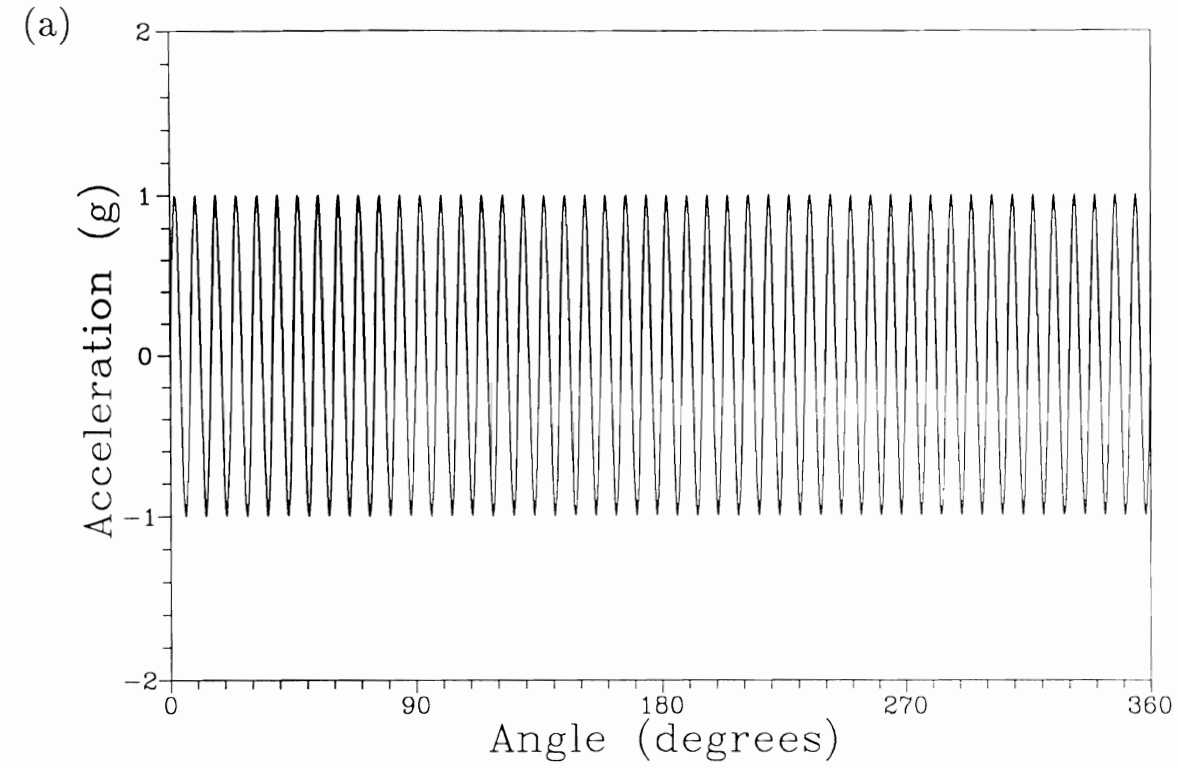

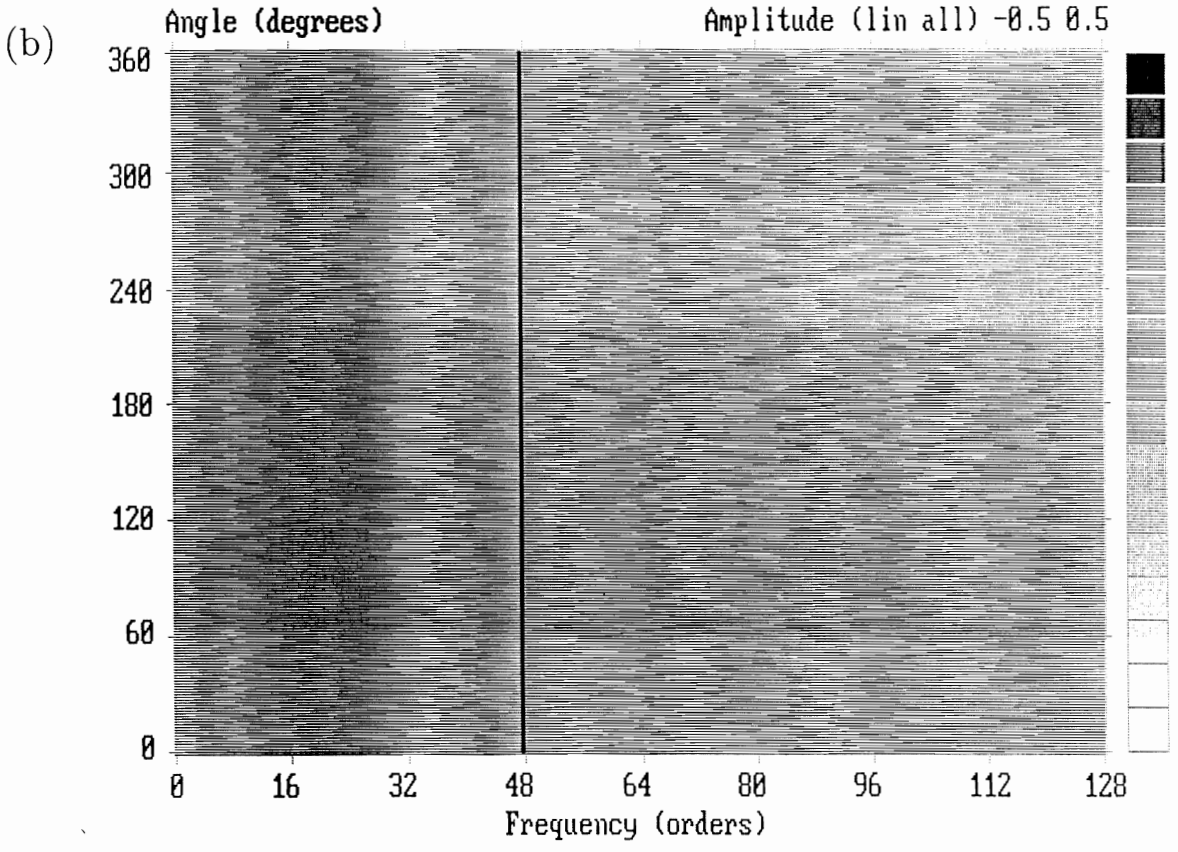

Figure 1 Example N1 Unmodulated sine wave

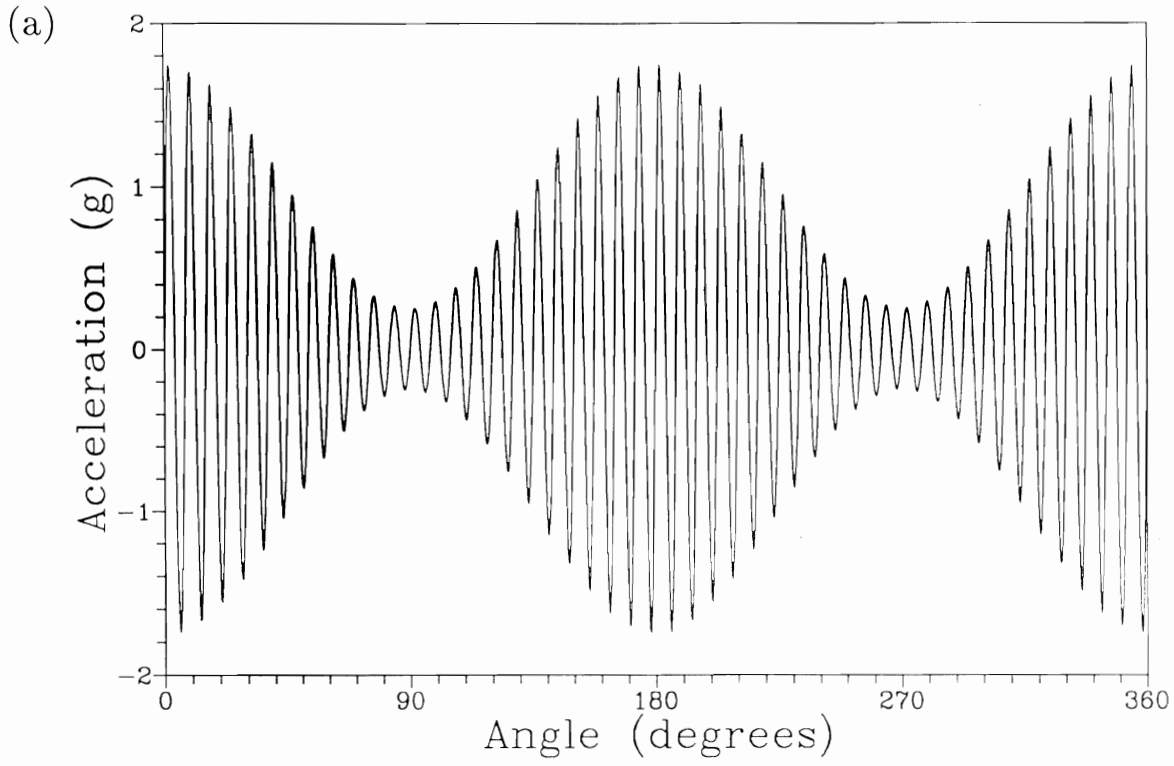

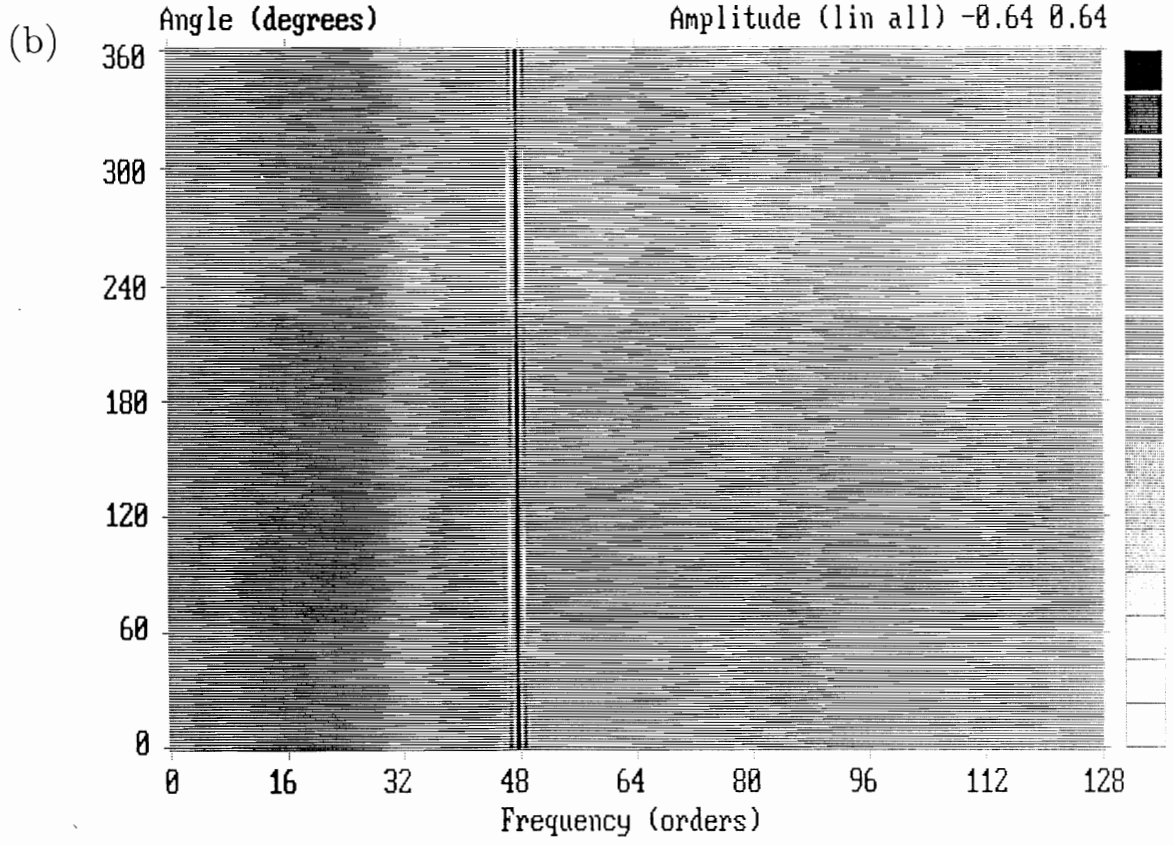

Figure 2 **Example N2** Amplitude modulated sine wave

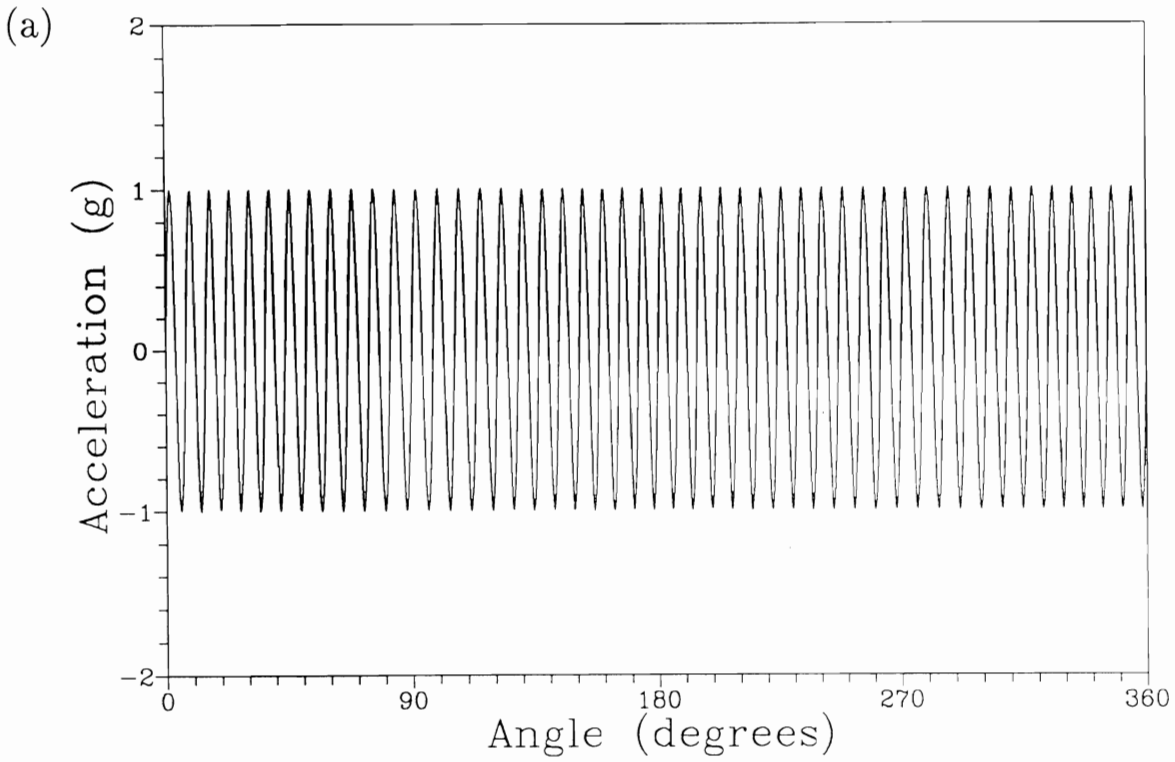

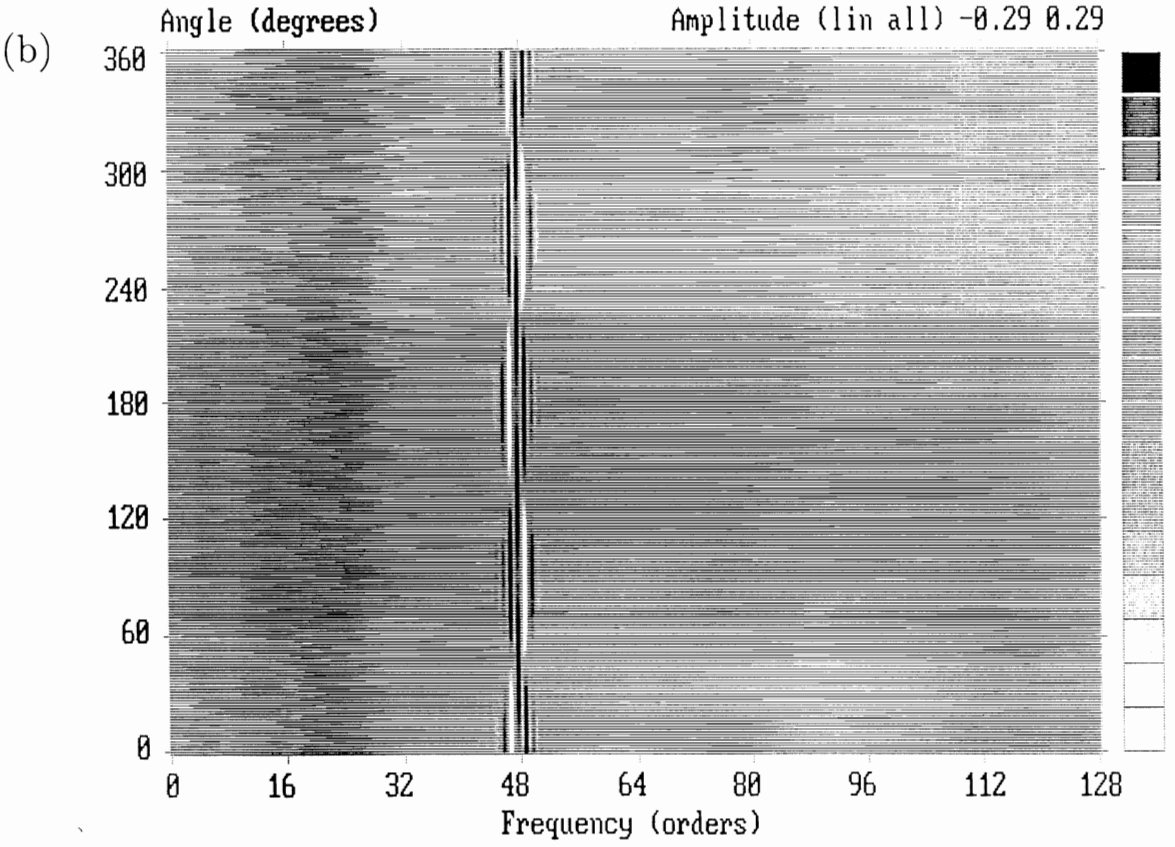

Figure 3 **Example N3** Phase modulated sine wave

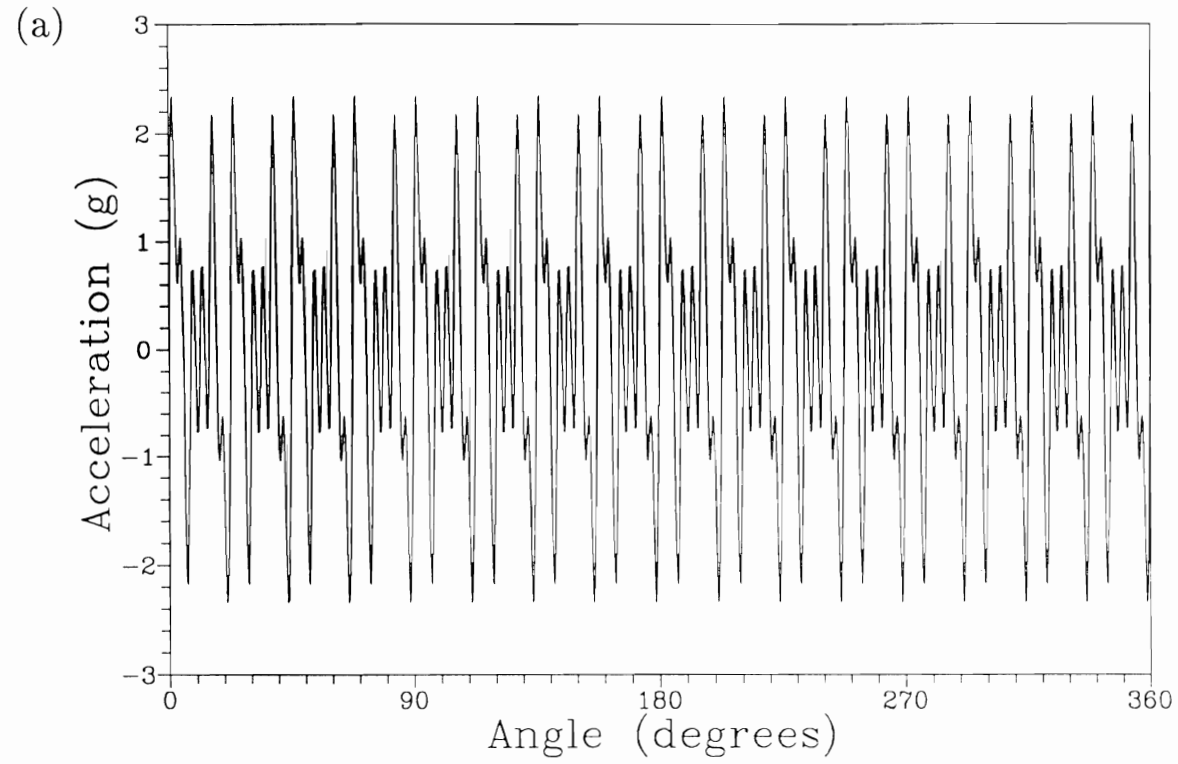

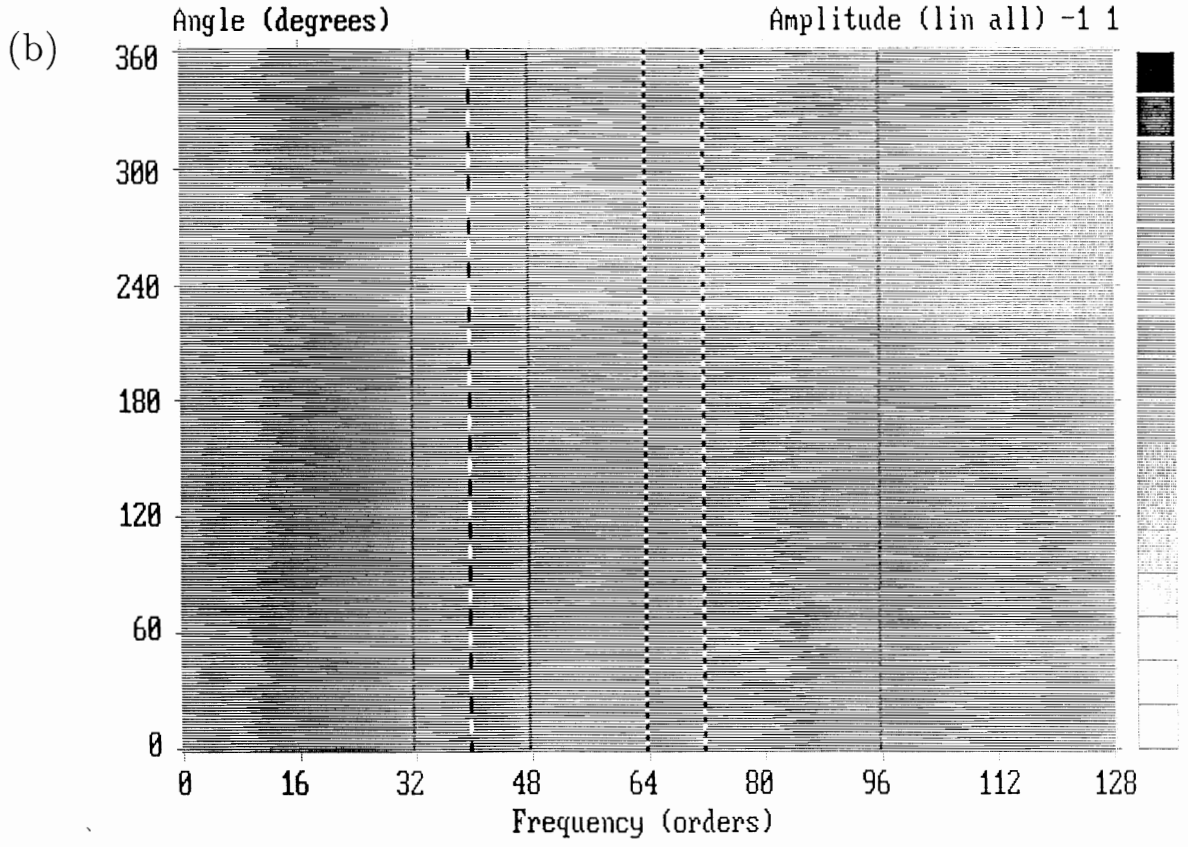

Figure 4 Example N4 Sum of sine waves

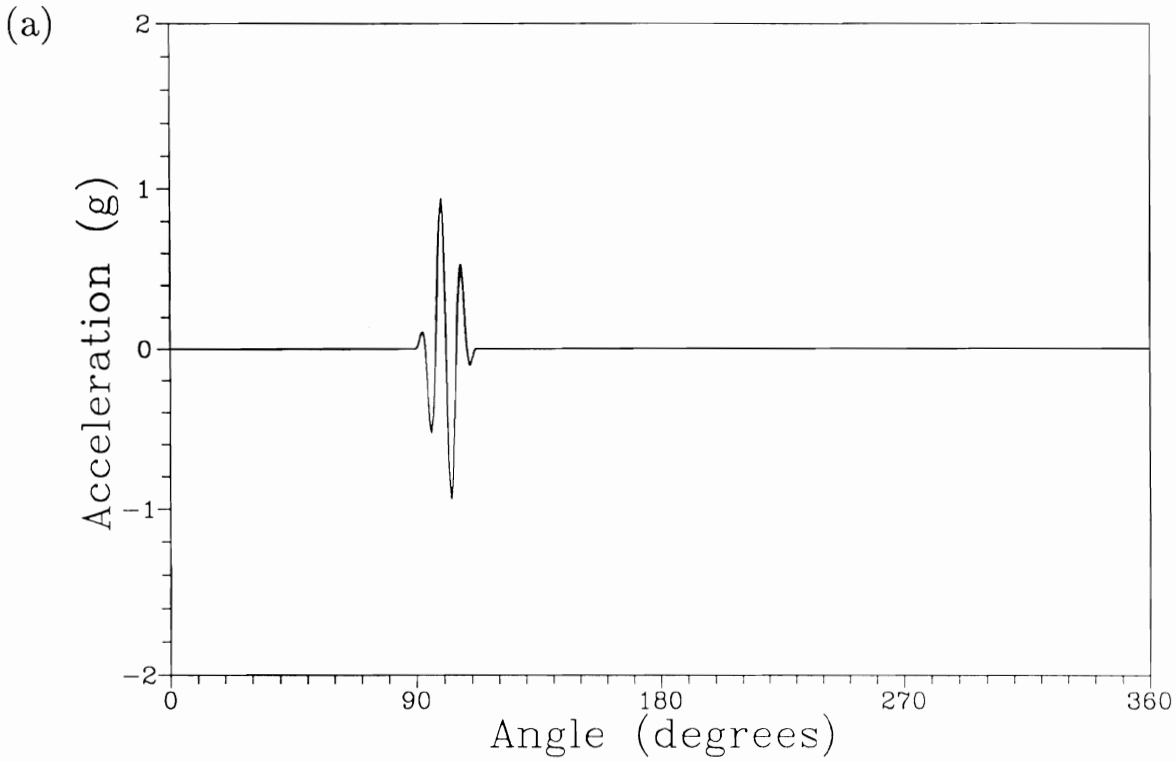

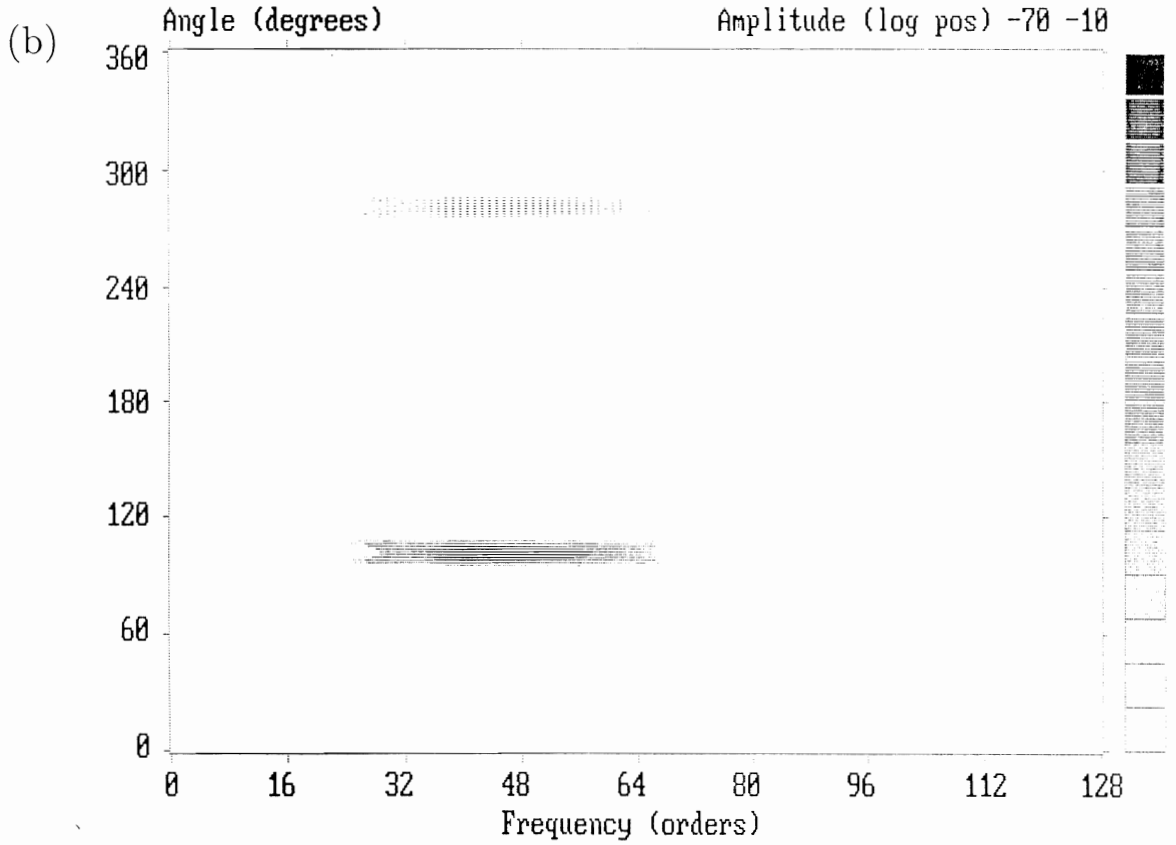

Figure 5 Example N5 Tone burst

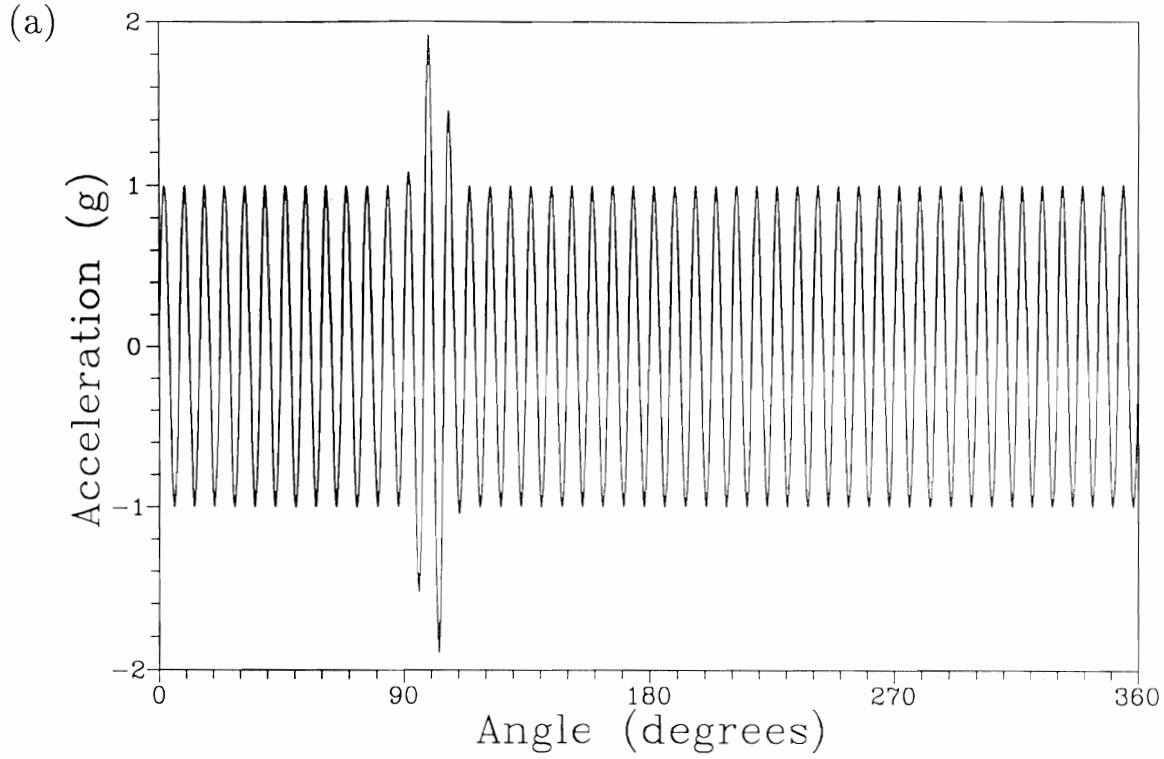

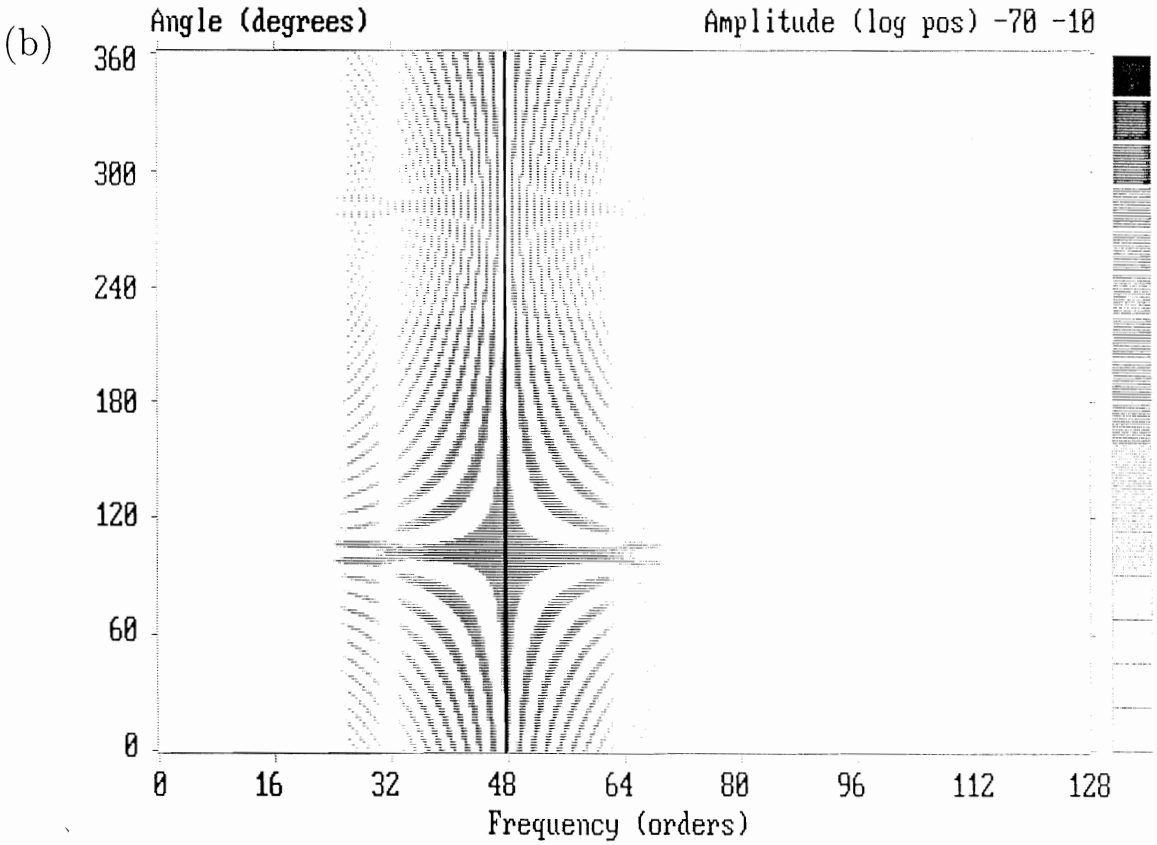

Figure 6 Example N6 Sum of tone burst and sine wave

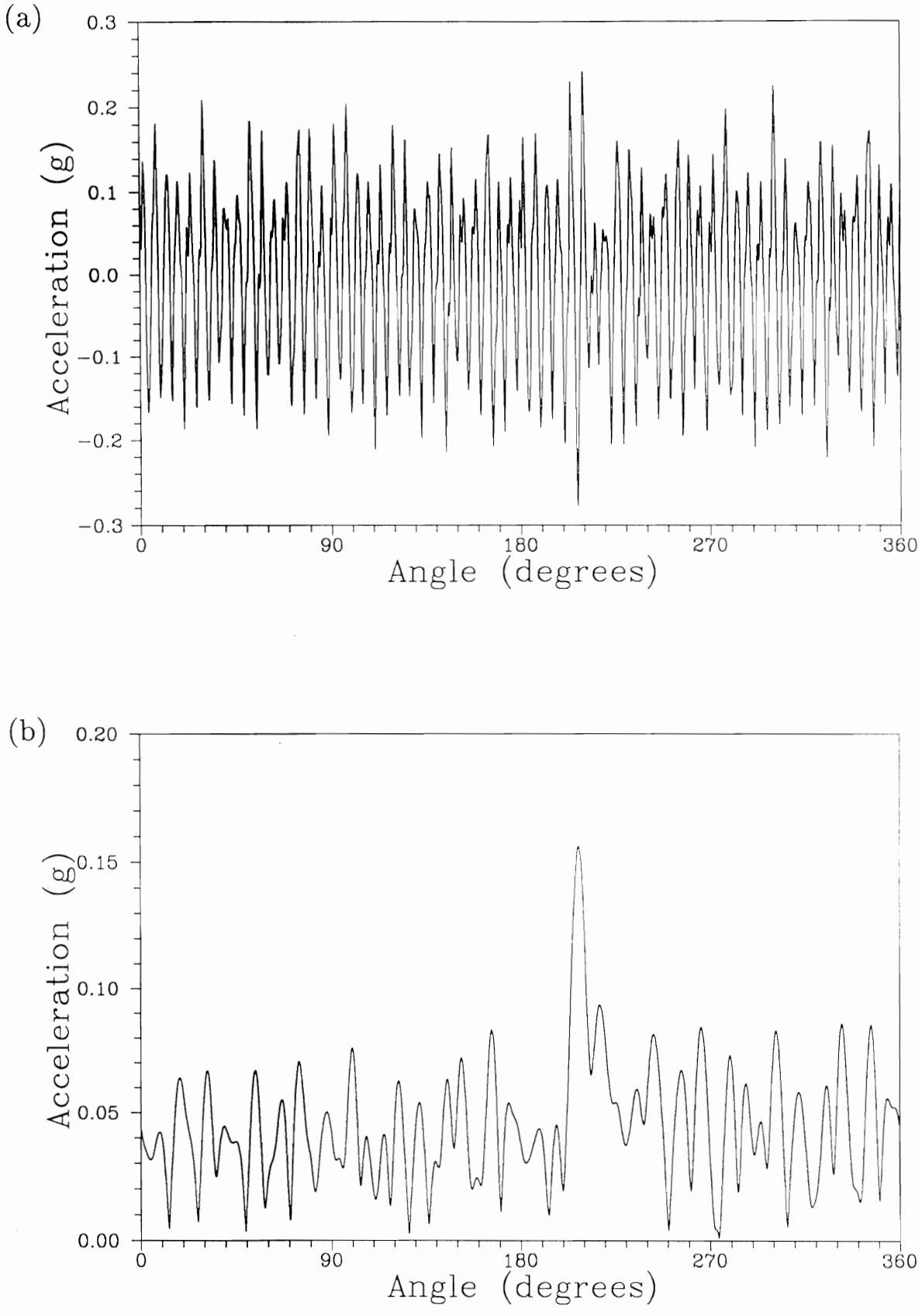

Figure 7 Example E1 Ball mill gearbox

(c)

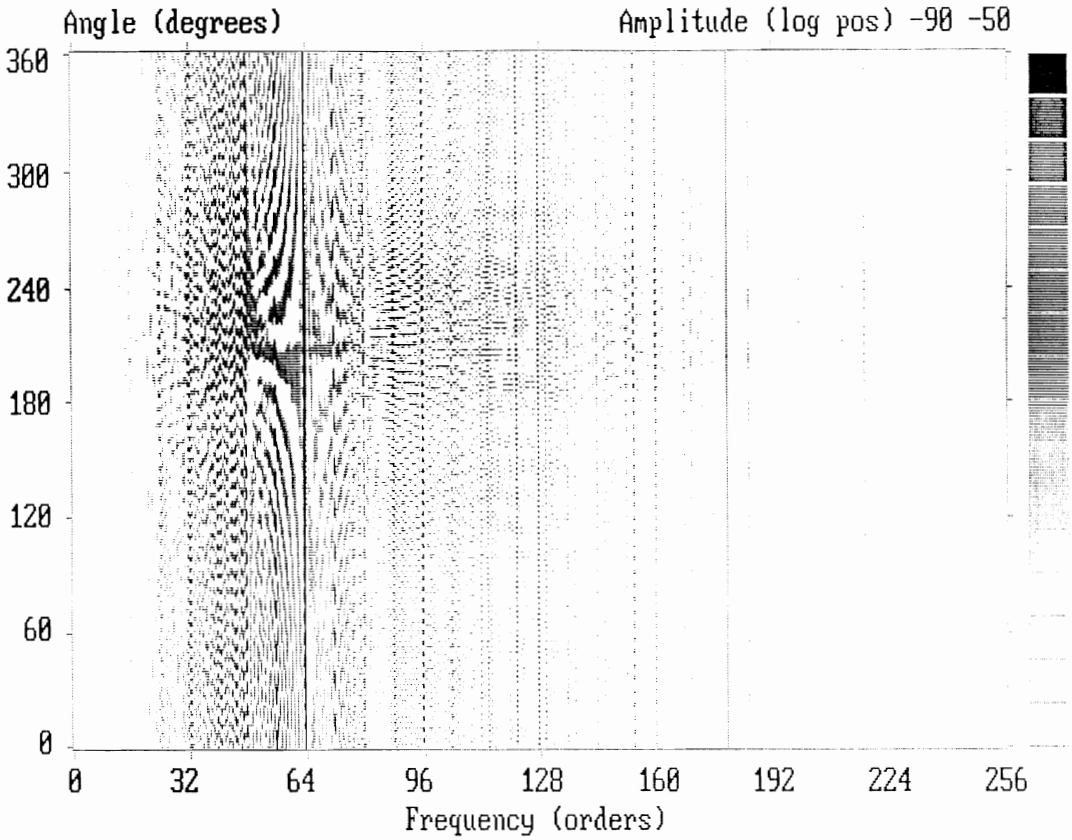

(d)

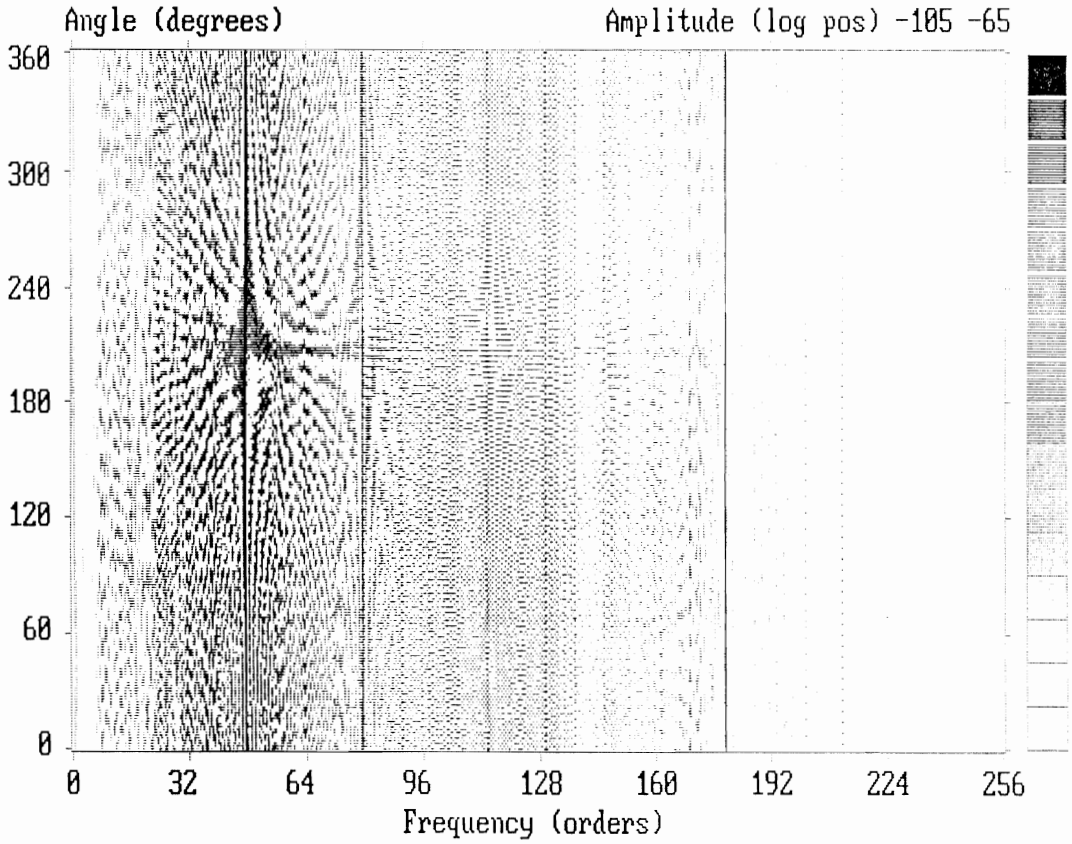

Figure 7 Example E1 Ball mill gearbox

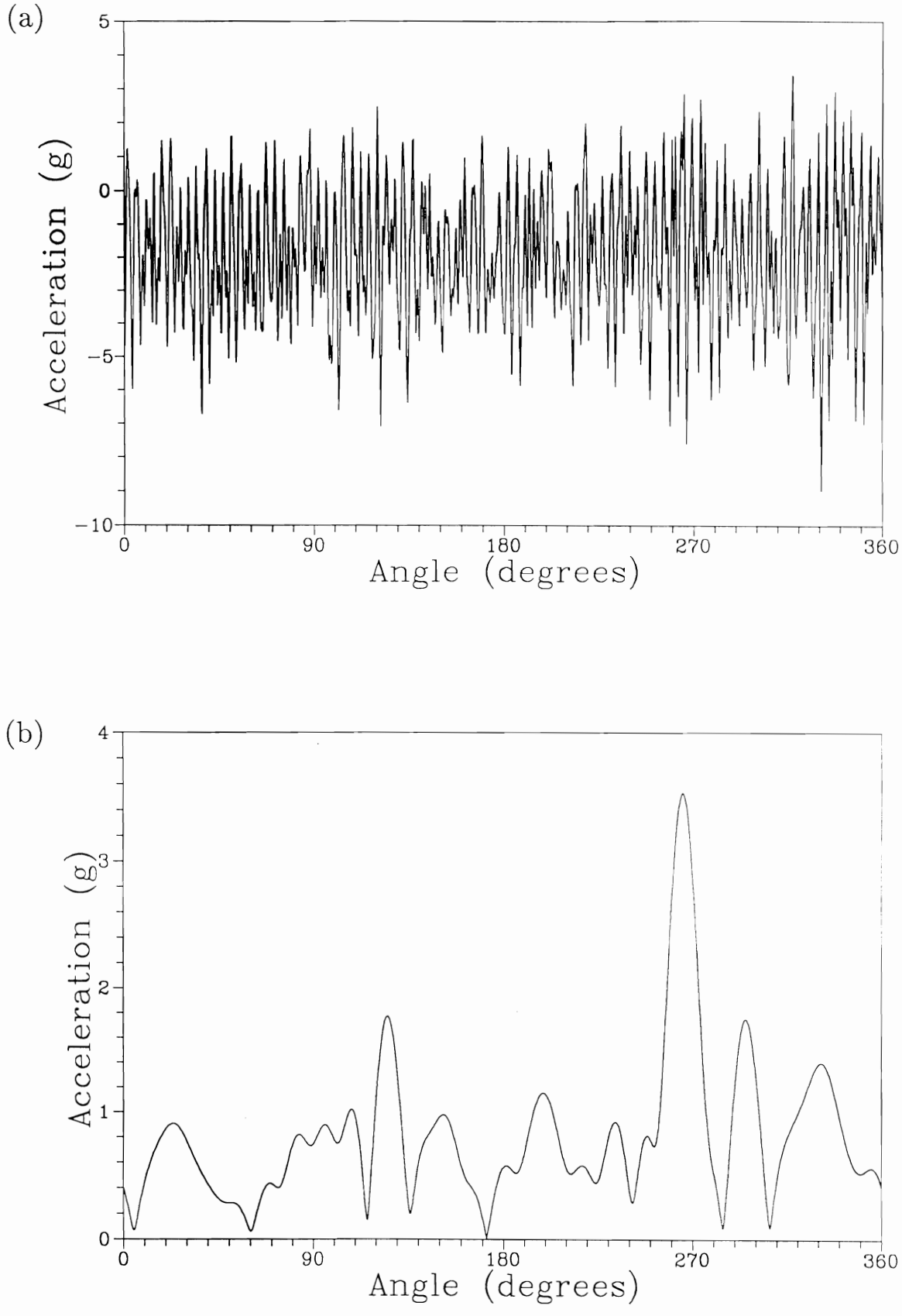

Figure 8 Example E2 Helicopter spiral bevel gear

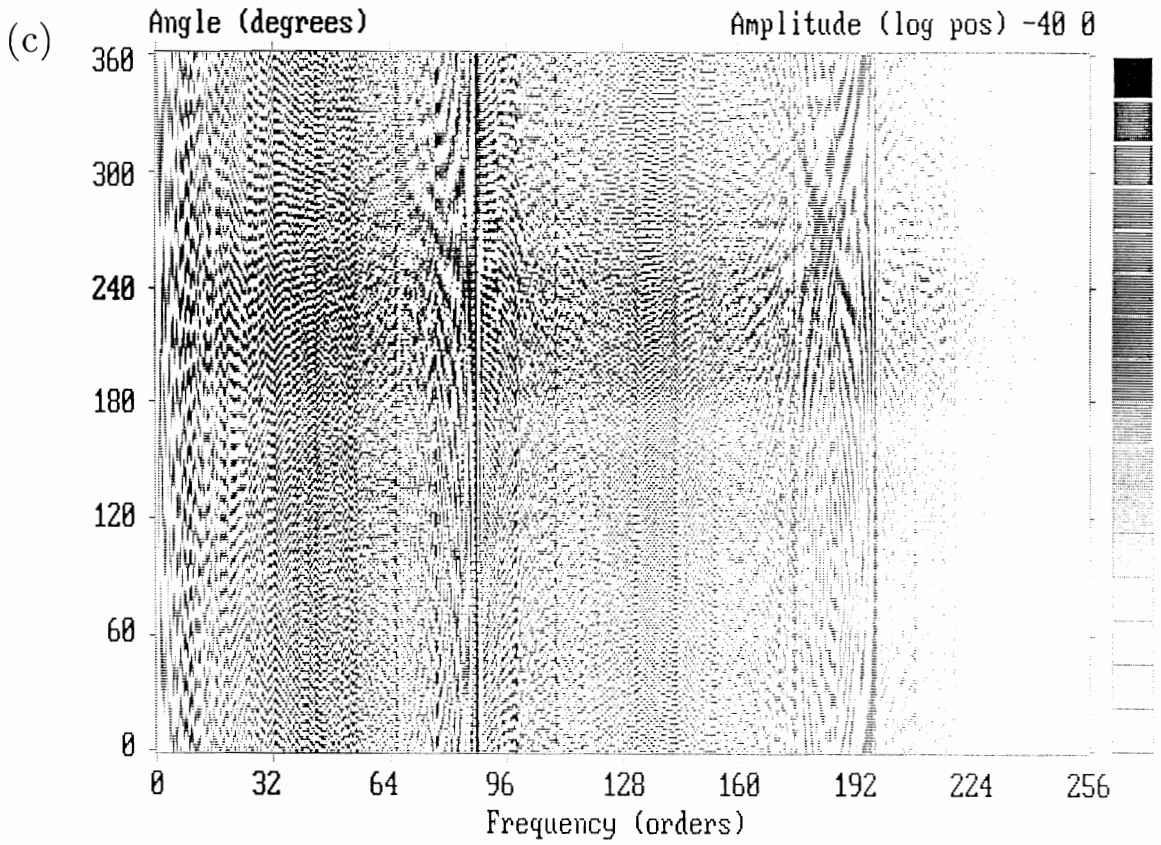

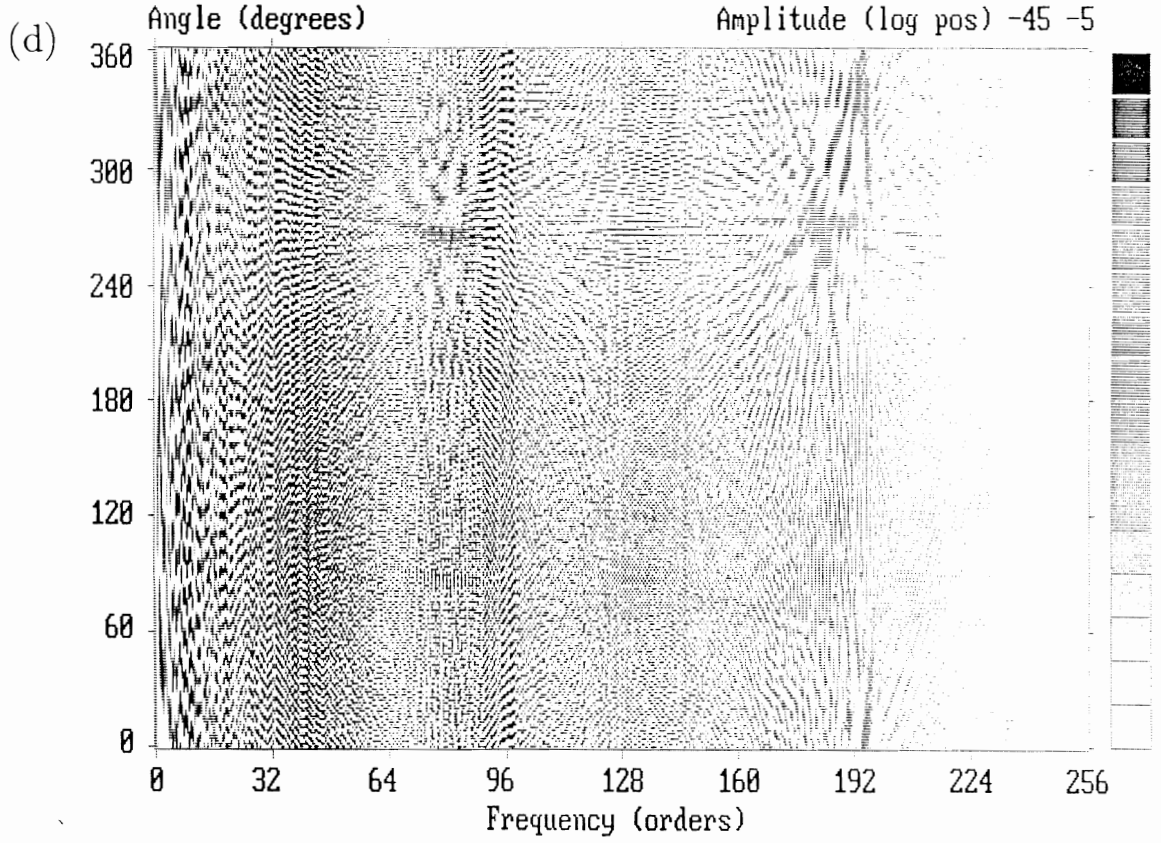

Figure 8 Example E2 Helicopter spiral bevel gear

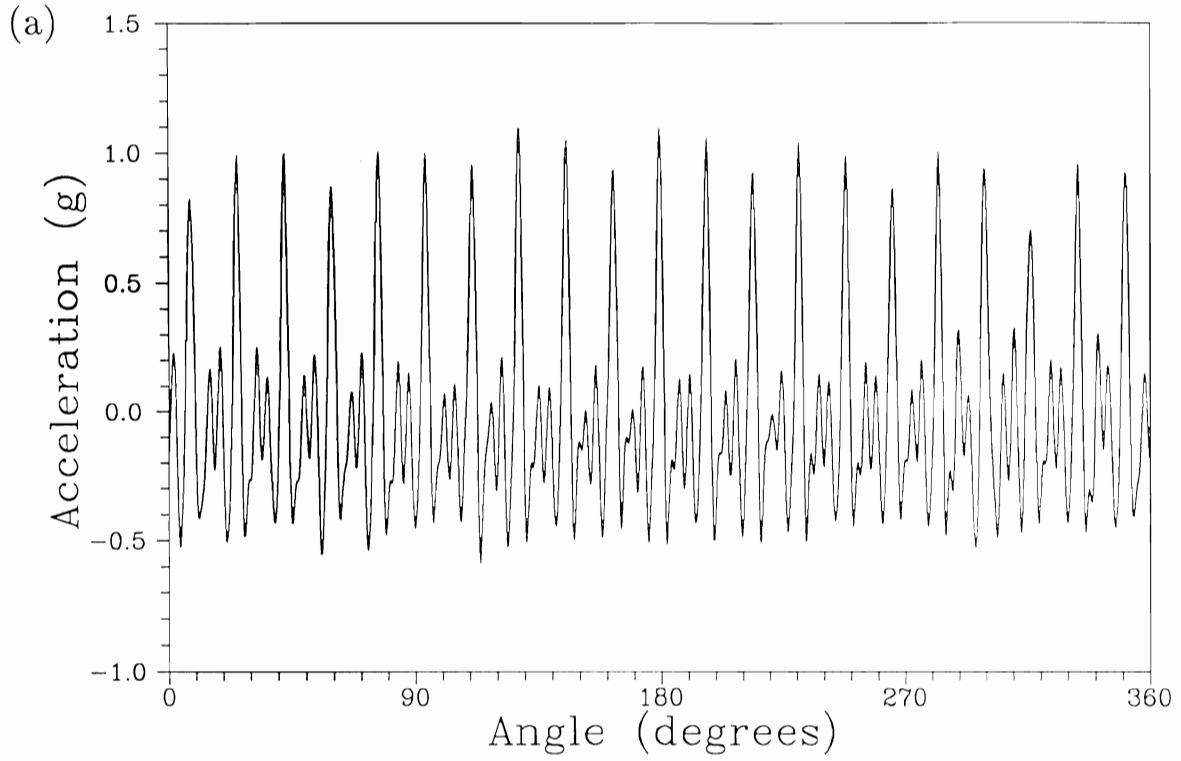

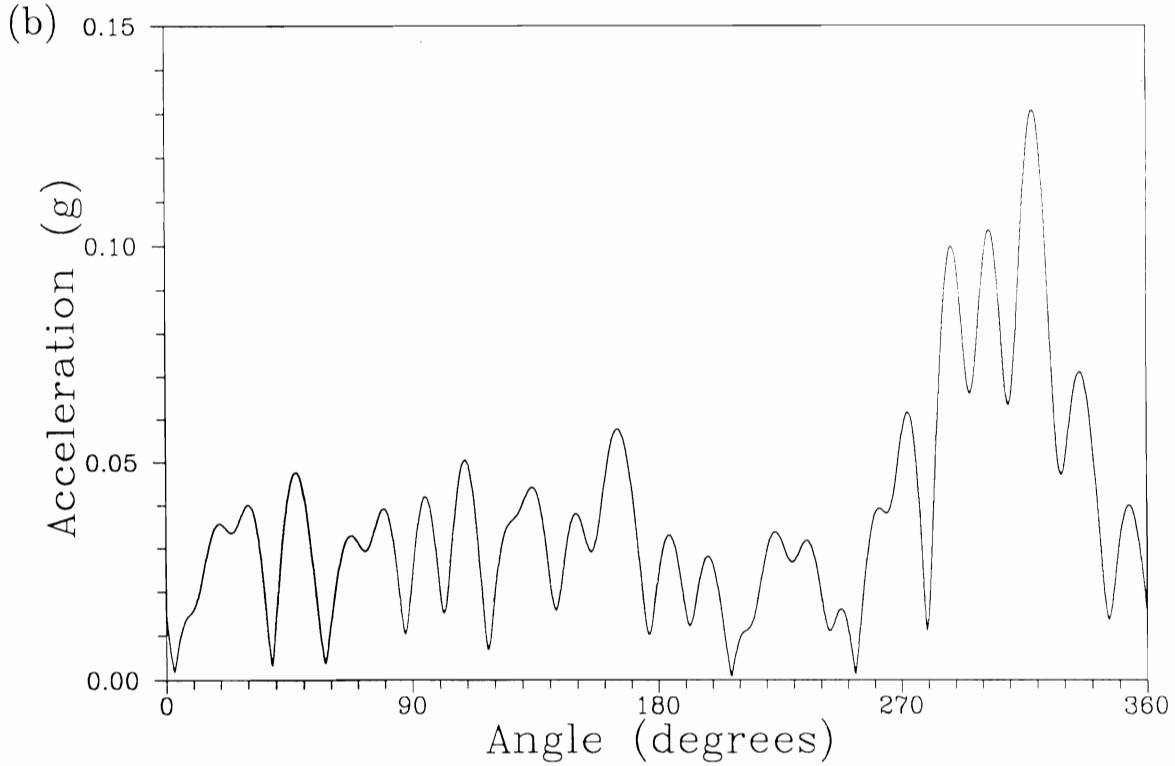

Figure 9 Example E3 Helicopter epicyclic planet gear

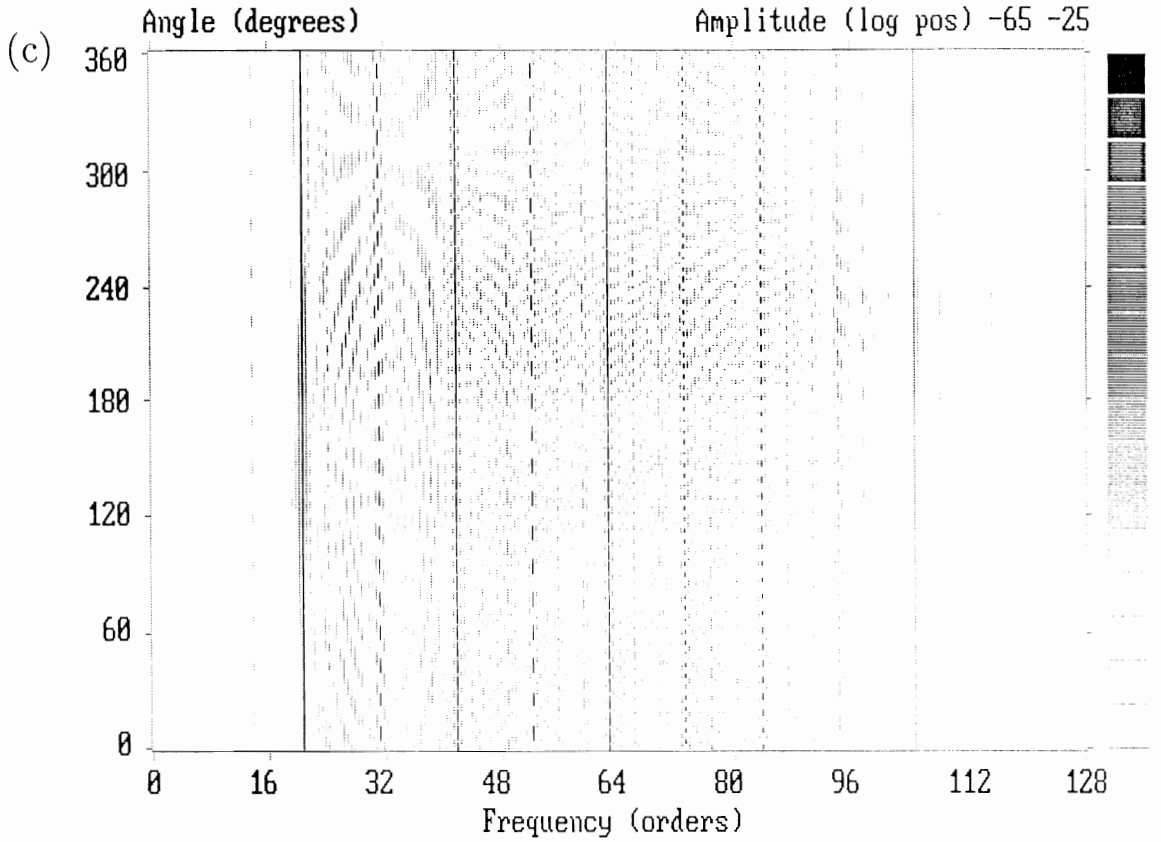

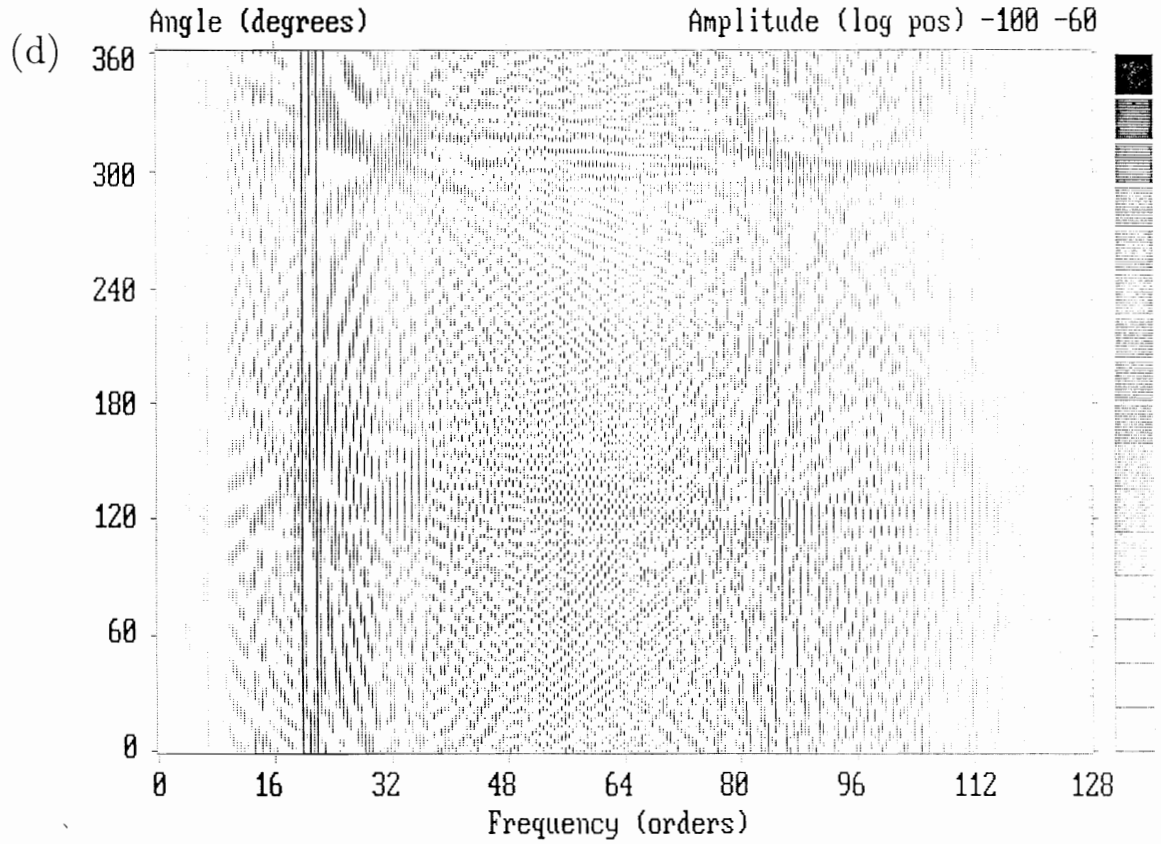

Figure 9 Example E3 Helicopter epicyclic planet gear